

1 **HDM-Plot: a plot dataset of plant communities across three-dimensional zonal**  
2 **vegetation in the Hengduan Mountains and adjacent regions, southwestern China**

3 Yili Jin, Liuyiyi Yang, Xiaofei Hu, Chen Yang, Haojun Xia, Ying Hou, Kai Wu, Shaolin Shi,  
4 Xingxing Mao, Jian Ni

5 College of Life Sciences, Zhejiang Normal University, Jinhua 321004, China

6 Correspondence: Xingxing Mao (xyz1314@zjnu.edu.cn); Jian Ni (nijian@zjnu.edu.cn).

7 **Abstract.** The Hengduan Mountains (HDM) constitute one of the world's richest biodiversity  
8 regions and are designated as a top-tier priority for ecological conservation. Vegetation  
9 investigations can help with the design and implementation of biodiversity conservation in this  
10 region. Here we present the HDM-Plot, a plot-based vegetation dataset compiled from 314 plots  
11 surveyed during four campaigns between 2022 and 2024 across the Hengduan Mountains and  
12 adjacent regions, spanning across major vegetation types from lowland dry-hot valleys to alpine  
13 areas ~~in-spanning~~ altitudes of 754–4,932 m. Each plot records detailed species-level information,  
14 including scientific name, growth form, life form, ~~abundance~~ number of individuals or clumps, plant  
15 height, diameter at breast height or at base, crown width, and coverage, along with geographic  
16 coordinates and hierarchical vegetation classification. In total, the dataset comprises 14,113  
17 individual records belonging to 1,127 species from 379 genera and 117 families. The dominant  
18 families are Rosaceae (133 species), Ericaceae (93), Fabaceae (66), Asteraceae (63), and Fagaceae  
19 (37), and the dominant genera are *Rhododendron* (75), *Berberis* (34), *Cotoneaster* (30), *Salix* (24),  
20 and *Quercus* (22), with composition varying among vegetation types. Growth forms are mainly  
21 composed of shrubs (46.0%), trees (27.3%), and herbs (23.6%). Herbs are dominated by perennial  
22 (92.1%), shrubs are mainly deciduous broadleaf (59.7%), and trees are primarily deciduous  
23 broadleaf (46.8%) and evergreen broadleaf (41.6%). Species richness ~~exhibits a unimodal pattern~~  
24 ~~with a mid-elevation peak, while,~~ growth forms, and life forms show clear elevational changes  
25 within the HDM-Plot dataset. Floristically, genus-level areal-types in the HDM-Plot dataset are  
26 dominated by temperate elements (54.1%), ~~and followed by~~ tropical ~~(35.4%) areal-type elements~~  
27 ~~(35.4%) are predominant~~. 314 plots can be assigned to three vegetation formation groups, 18  
28 vegetation formations, 142 alliance groups, 209 alliances, 238 association groups, and 299  
29 associations. The HDM-Plot dataset provides an updated and standardized baseline for quantitative

30 analyses of mountain vegetation, biodiversity assessment, and vegetation classification and  
31 mapping in southwestern China. Such information can be future used in the revisions of China's  
32 vegetation classification scheme and *Vegeography of China*. The dataset is available through the  
33 National Tibetan Plateau / Third Pole Environment Data Center (Jin et al., 2026;  
34 <https://doi.org/10.11888/Terre.tpdc.303394>).

## 35 **1 Introduction**

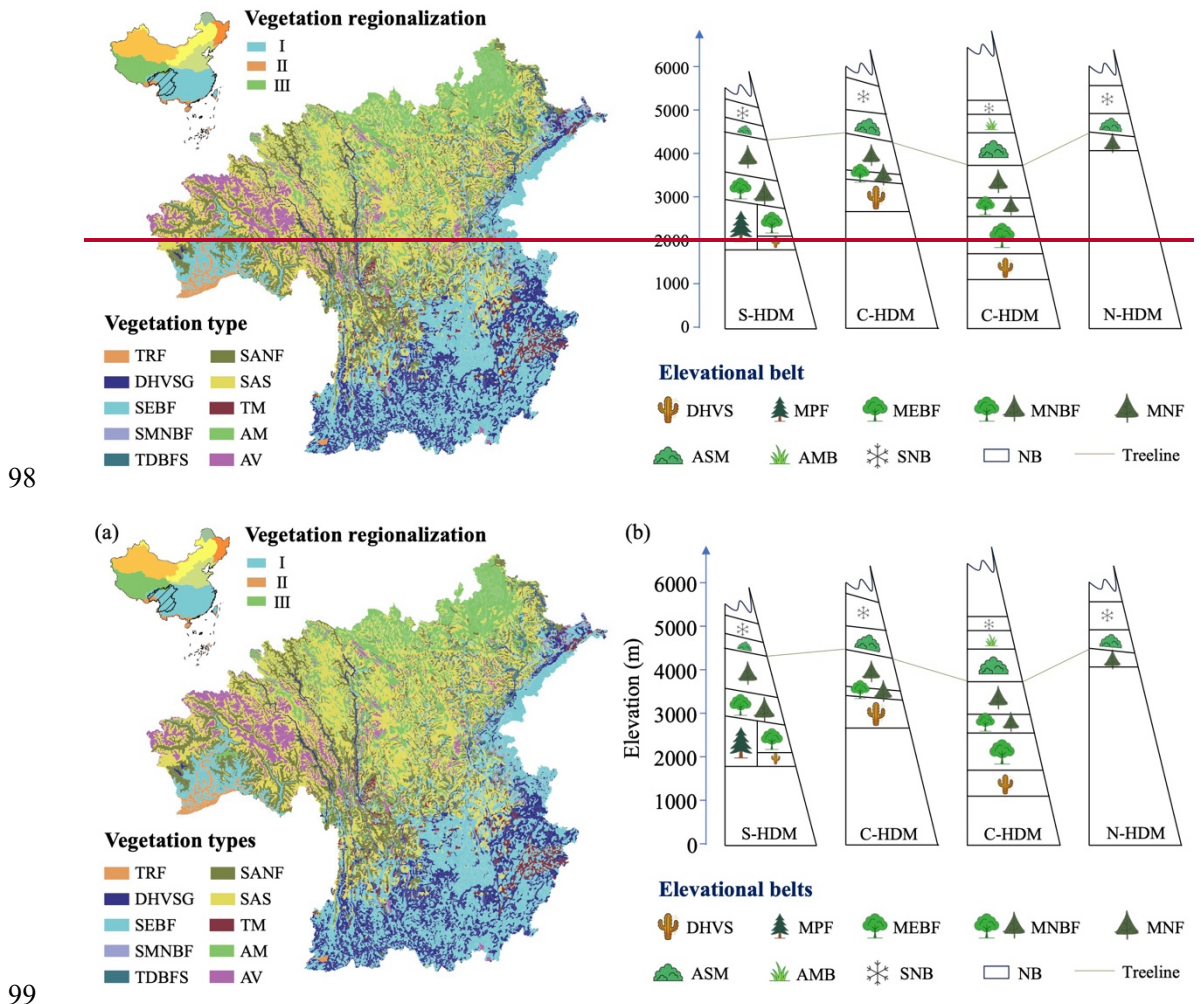
36 The Hengduan Mountains (HDM) form the core mountainous region in  
37 southwestern China and are recognized as one of the world's richest biodiversity  
38 hotspots and a global priority area for ecological conservation (Myers et al., 2000; Sloan  
39 et al., 2014). Located at the junction between the Tibetan Plateau and the Yangtze Block,  
40 the HDM represents a young and rapidly evolving orogenic belt shaped by ongoing  
41 tectonic uplift associated with Indian–Eurasian collision (Xing and Ree, 2017). Long-  
42 term mountain uplift, together with intense river incision, has generated exceptional  
43 topographic complexity, characterized by closely spaced north–south–oriented high  
44 mountains and deeply incised valleys (Integrated Scientific Expedition to Qinghai-  
45 Tibet Plateau, Chinese Academy of Sciences, 1997). As an ecotonal region linking  
46 subtropical lowlands to alpine highlands, the HDM is affected by the southwest and  
47 southeast monsoons as well as mesoscale atmospheric systems (Wu et al., 2012; Zhang  
48 et al., 2024). These interacting geological and climatic processes create strong  
49 environmental heterogeneity, supporting abundant biodiversity, significant spatial  
50 differentiation of ecosystems, and complex vegetation distribution (Liang et al., 2018;  
51 Ding et al., 2020; He et al., 2020). Consequently, robust characterization of species  
52 composition, community structure, and vegetation zonation in the HDM is essential for  
53 biodiversity conservation and sustainable development, thereby provides key empirical  
54 support for advancing studies of global mountain biogeography and ecology.

55 Vegetation represents the most visible and distinctive ecological feature of a region,  
56 and plot-based plant community data provide the fundamental basis for documenting  
57 vegetation composition and distribution patterns, as well as for the compilation of the

58 *Vegeography*—a series of monographs that describe detailed species composition,  
59 structures, functions, environmental settings, and distribution of a set of plant  
60 communities and/or their combinations for each vegetation type, using community data  
61 from vegetation survey (Fang et al., 2020; Wang et al., 2020; Sabatini et al., 2021). Over  
62 recent decades, extensive vegetation surveys have been conducted across the HDM and  
63 its adjacent mountains and plateaus, including those in the First (1970–1990) and  
64 Second (2018–2024) Tibetan Plateau Scientific Expeditions, and numerous regional  
65 surveys (the late 20<sup>th</sup> to the early 21<sup>st</sup> Century). These efforts have substantially  
66 advanced theoretical knowledge of floristic composition (Li, 1988; Shen et al., 2004;  
67 Xu et al., 2014; Yu et al., 2020), community structure (Sherman et al., 2008; Xu et al.,  
68 2008; Sun et al., 2017), vegetation distribution (Yao et al., 2010; Liang et al., 2018; Wu  
69 and Yu, 2020; Zhang et al., 2023), eco-geographical regionalization (Zheng and Yang,  
70 1987; Yang and Zheng, 1989; Chi et al., 2019), and vegetation modeling (He et al., 2020;  
71 Yin et al., 2020), with sustained attention to dry-hot valley vegetation (Jin and Ou, 2000;  
72 Jin, 2002; Liu et al., 2016a, b; Yang J D et al., 2016; Yang Y et al., 2016).

73 Existing plot surveys consistently indicate significant horizontal differentiation  
74 and elevational turnover in HDM vegetation (Editorial Committee of Vegetation Map  
75 of China, the Chinese Academy of Sciences, 2007a, b). ~~Vegetation across the HDM~~  
76 ~~spans three regions i~~In the vegetation regionalization scheme of China, the study region  
77 spans three vegetation regionalization units: ~~the dominated one is~~ the subtropical  
78 evergreen broadleaf forest region, ~~while a small area in the northwestern sector is~~  
79 ~~transitioned to~~ the Qinghai-Xizang Plateau alpine vegetation region, and ~~the western~~  
80 ~~margin is~~ the tropical monsoon rain forest and rain forest region (Fig. 1a; Table S1;  
81 Editorial Committee of Vegetation Map of China, the Chinese Academy of Sciences,  
82 2007b). Across the region, ~~From from~~ the southeast toward the northwest, vegetation  
83 types shifts from subtropical evergreen broadleaf forests and dry-hot valley shrubby  
84 grasslands to subalpine needleleaf forests, subalpine shrublands, and alpine meadows  
85 (Fig. 1a; Table S1; Editorial Committee of Vegetation Map of China, the Chinese  
86 Academy of Sciences, 2007a). Along elevational gradients, vegetation belt spectra  
87 typically transition from the dry-hot valley shrubland belt through the belts of

88 mountains evergreen broadleaf forest, mixed needleleaf and broadleaf forest, and  
 89 needleleaf forest, to the belts of alpine shrubland and meadow, alpine meadow, and the  
 90 nival (Fig. 1b; Zheng, 1988). Despite a large number of community plot data  
 91 accumulated by earlier surveys, many datasets remain difficult to integrate for synthesis  
 92 due to extended temporal spans, limited accessibility of original records, heterogeneous  
 93 study designs, as well as inconsistent taxonomic and classification frameworks across  
 94 campaigns. Meanwhile, vegetation on the Tibetan Plateau including the HDM has been  
 95 reshaped under increasing climate change and human activities (Zhang et al., 2015;  
 96 Piao et al., 2019), highlighting the need for updated, standardized, and openly available  
 97 plot-based plant community data.



100 **Figure 1. Horizontal (a) and elevational (b) spatial patterns of vegetation distribution in the**  
 101 **Hengduan Mountains (HDM) and adjacent regions—the HDM-Plot study region. The upper-left**  
 102 **inset map shows the location of the HDM in China and the vegetation regionalization**  
 103 **was obtained from the *Vegetation Regionalization Map of China* (Editorial Committee of Vegetation**

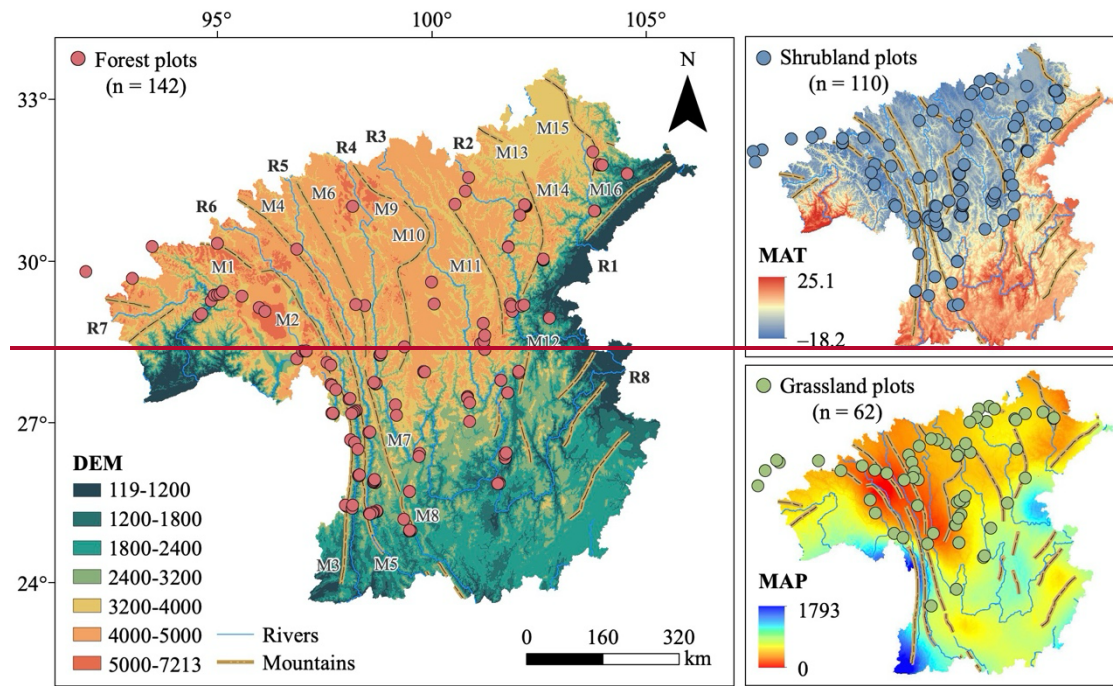
104 Map of China, the Chinese Academy of Sciences, 2007b). I, subtropical evergreen broadleaf forest  
105 region; II, tropical monsoon rain forest and rain forest region; and III, Qinghai-Xizang Plateau alpine  
106 vegetation region. ~~The left panel exhibits the vegetation~~ Vegetation types were extracted from the  
107 *1:1,000,000 Vegetation Map of the People's Republic of China* (Editorial Committee of Vegetation  
108 Map of China, the Chinese Academy of Sciences, 2007a). The original 35 vegetation formations  
109 were aggregated into 10 categories based on climatic zones, community structures, and ecological  
110 function. TRF, tropical rain forest; DHVSG, dry-hot valley shrubby grassland; SEBF, subtropical  
111 evergreen broadleaf forest; SMNBF, subtropical mountains mixed needleleaf and broadleaf forest;  
112 TDBFS, temperate deciduous broadleaf forest and shrubland; SANF, subalpine needleleaf forest;  
113 SAS, subalpine shrubland; TM, temperate meadow; AM, alpine meadow; and AV, alpine cushion  
114 and sparse vegetation, and bare land. Elevational vegetation belt spectra~~The right panel presents~~  
115 elevational belts (revised after Zheng, 1988) for the southern (S-HDM), central (C-HDM), and  
116 northern (N-HDM) sectors of the Hengduan Mountains were revised after Zheng (1988). DHVS,  
117 dry-hot valley shrubland belt; MPF, mountains *Pinus* forest belt; MEBF, mountains evergreen  
118 broadleaf forest belt; MNBF, mountains mixed needleleaf and broadleaf forest belt; MNF,  
119 mountains needleleaf forest belt; ASM, alpine shrubland and meadow belt; AMB, alpine meadow  
120 belt; SNB, subnival belt; and NB, nival belt.

121 To provide an up-to-date baseline of vegetation composition and spatial patterns  
122 in the HDM and adjacent regions, we conducted four large-scale surveys between 2022  
123 and 2024 along the major mountains and valleys, spanning tropical, subtropical, and  
124 temperate zones and extending into subalpine and alpine environments, in accordance  
125 with the horizontal and vertical zonation. We surveyed 314 plant community plots and  
126 integrated all field records into a standardized plot-based vegetation dataset, HDM-Plot.  
127 It documents plant species composition and taxonomic attributes and supports a  
128 consistent vegetation classification across the region. The HDM-Plot dataset provides  
129 a contemporary and standardized baseline for plant community study and long-term  
130 monitoring of vegetation, and serves as a vital reference for biodiversity conservation,  
131 vegetation restoration, and sustainable development. It also offers empirical support for  
132 revising of the China's vegetation classification scheme (Guo et al., 2020) and the  
133 compilation of the *Vegegraphy of China* (Fang et al., 2020).

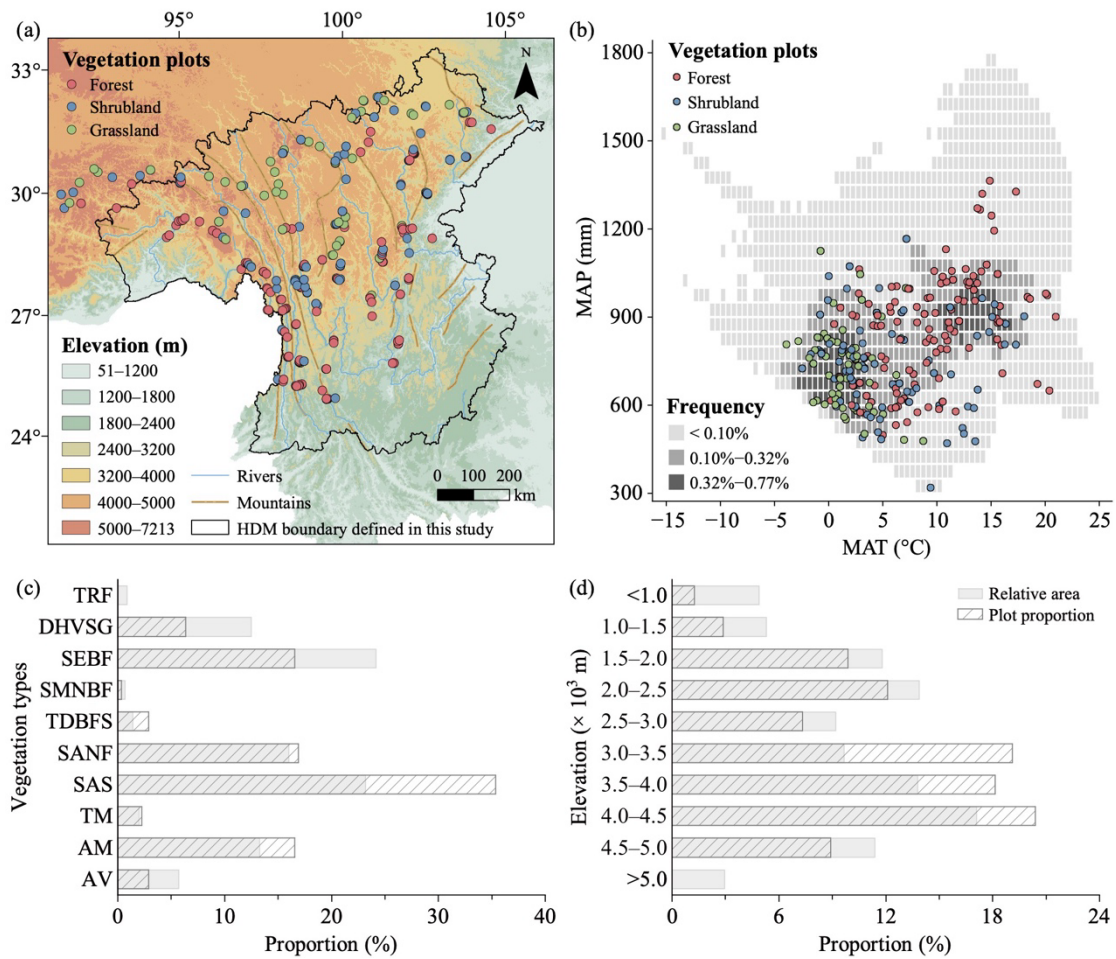
## 134 2 Study area

135 The HDM covers a broad geographical extent, and their spatial boundaries can  
136 vary slightly among studies depending on research objectives. Here we define the  
137 study, we use the HDM boundary (24.08°–34.32° N, 93.13°–106.16° E, 119–7,213 m;

138 ~~Fig. 2a) as extending from 24.08° to 34.32° N and from 93.13° to 106.16° E, with~~  
139 ~~elevations ranging from 119 to 7,213 m (Fig. 2), following the standard of two studies~~  
140 ~~(Yu et al., (1989); and Zhang et al., (1997) as the geographical core of the study region.~~  
141 ~~Because of the continuity of regional topography, the gradual transition of vegetation~~  
142 ~~belts, and the practical arrangement of survey routes, the actual survey extent included~~  
143 ~~adjacent regions along the southeastern and northwestern margins (Fig. 2a). These~~  
144 ~~peripheral plots record important vegetation transitions from the HDM toward adjacent~~  
145 ~~regions, and were therefore retained. Unless otherwise specified, the “HDM-Plot study~~  
146 ~~region” in this manuscript refers to the HDM and adjacent regions covered by our field~~  
147 ~~surveys, rather than to the HDM sensu stricto.~~ The region exhibits an overall increase  
148 in elevation from the southeast toward the northwest and is characterized by a series of  
149 north–south–oriented mountains and deeply incised valleys. Climatically, the HDM-  
150 Plot study region spans tropical, subtropical, temperate, and alpine zones, with mean  
151 annual temperature ranging from –18.2 to 25.1 °C. Warmer conditions are concentrated  
152 in the dry-hot valleys and lower subtropical mountains in the southeast, and in the  
153 tropical rainforests along the western margin, while much lower temperatures occur  
154 across the highlands toward the northwest. Mean annual precipitation across the region  
155 varies but is generally lower (0–1,793 mm), and relatively humid conditions are mainly  
156 associated with the southwestern and southeastern margins (Fig. 2**b**).



157



158

159 **Figure 2.** Distribution-Spatial (a), climatic (b), vegetation-type (c), and elevational (d) coverage of  
 160 vegetation plots in the Hengduan Mountains HDM-Plot dataset. Vegetation plots of different  
 161 vegetation types (forest, shrubland, and grassland), often overlapped in one location, were separately

162 ~~drawn on different maps. n indicates the number of plots. Digital elevation model~~Elevation data  
163 ~~(DEM, m) was were~~ derived from the SRTM 90 m dataset (Farr et al., 2007) and resampled into 1  
164 km grid cells. ~~Mountain and river data were obtained from the Digital Mountain Map of China~~  
165 ~~Dataset (Nan et al., 2015) and Natural Earth (https://www.naturalearthdata.com, last access: 12~~  
166 ~~March 2026), respectively.~~ Mean annual temperature (MAT, °C) and mean annual precipitation  
167 (MAP, mm) were derived from ~~a 1 km monthly climate dataset for China covering 1991–2020 (Hu~~  
168 ~~et al., 2025).~~ Grey cells in panel (b) indicate the frequency of MAT–MAP combinations among all  
169 1 km grid cells within the study boundary, based on two-dimensional bins of 0.5 °C for MAT and  
170 50 mm for MAP. In panels (c) and (d), grey bars indicate the relative area of each vegetation type  
171 and elevational belt within the study region, and hatched bars represent the proportion of surveyed  
172 plots within each group. Vegetation types were extracted from the *1:1,000,000 Vegetation Map of*  
173 *the People's Republic of China* (Editorial Committee of Vegetation Map of China, the Chinese  
174 Academy of Sciences, 2007a). TRF, tropical rain forest; DHVSG, dry-hot valley shrubby grassland;  
175 SEBF, subtropical evergreen broadleaf forest; SMNBF, subtropical mountain mixed needleleaf and  
176 broadleaf forest; TDBFS, temperate deciduous broadleaf forest and shrubland; SANF, subalpine  
177 needleleaf forest; SAS, subalpine shrubland; TM, temperate meadow; AM, alpine meadow; and AV,  
178 alpine cushion vegetation, alpine sparse vegetation, and bare land.~~the monthly climatological~~  
179 ~~standard normals at 2,152 meteorological stations across China in 1981–2010 (China~~  
180 ~~Meteorological Data Service Centre, http://data.cma.cn, last access: 8 June 2024), and interpolated~~  
181 ~~into 1 km grid cells by using the thin plate smoothing spline in ANUSPLIN version 4.4. Mountain~~  
182 ~~data were extracted from the Digital Mountain Map of China Dataset (Nan et al., 2015). Major~~  
183 ~~mountains include: M1, Nyenchen Tanglha Mountain (Mt); M2, Boshulaling Mt; M3, Gaoligong~~  
184 ~~Mt; M4, Taniantaweng Mt; M5, Nushan Mt; M6, Mangkang Mt; M7, Yunling Mt; M8, Diancang~~  
185 ~~Mt; M9, Que'er Mt; M10, Shaluli Mt; M11, Daxue Mt; M12, Xiaoxiangling Mt; M13, Bayan Har~~  
186 ~~Mt; M14, Qionglai Mt; M15, Minshan Mt; and M16, Longmen Mt. River data were extracted from~~  
187 ~~the Natural Earth (https://www.naturalearthdata.com, last access: 12 March 2026). Major rivers~~  
188 ~~include: R1, Min River; R2, Dadu River; R3, Yalong River; R4, Jinsha River; R5, Lancang River;~~  
189 ~~R6, Nu River; R7, Yarlung Tsangpo River; and R8, Yangtze River.~~

## 190 **3 Materials and Methods**

### 191 **3.1 Vegetation survey**

192 Field surveys were conducted during four campaigns in March 2022, May–June  
193 2022, May–June 2023, and June 2024. May–June was selected as the primary survey  
194 time because most species across elevational belts in the region have developed  
195 diagnostic vegetative structures and even many have begun flowering, enabling reliable  
196 identification. In addition, it coincides with the transition from the dry to the wet season  
197 when precipitation is still relatively low and field accessibility is generally high. An  
198 additional survey in March 2022 targeted dry-hot valley vegetation, where phenological

199 development occurs earlier under warm and relatively arid conditions.

200 To capture the major vegetation belts and transition zones shaped by the regional  
201 mountain–valley and climatic system gradients, we adopted a coverage-oriented field  
202 sampling design. plots Plots were set up across representative mountains and valleys of  
203 the HDM and adjacent regions along various longitudinal, latitudinal, and elevational  
204 gradients. The survey aimed to cover major vegetation physiognomic types,  
205 representative mountain–valley systems, and local transitions among forest, shrubland,  
206 and grassland communities. with Field logistics and, road accessibility, and terrain  
207 conditions were also considered during plot selection. Plot size was determined  
208 following community physiognomy and stand heterogeneity. The sizes of Ggrassland  
209 plots were mainly 1 m × 1 m (91.9% of grassland plots), of shrubland plots were mainly  
210 5 m × 5 m (70.0%), and of forest plots were mainly 10 m × 10 m (56.3%) or 10 m × 20  
211 m (29.6%). Local adjustments in plot size were made because of terrain constraints,  
212 especially slope, and field operability in complex mountain environments. The  
213 dominant plot size covered broad spatial and elevational ranges within the surveyed  
214 distribution of their corresponding vegetation types (Fig. S1; Table S2). Forest plots  
215 were typically 10 m × 10 m to 20 m × 20 m, shrubland plots 2 m × 2 m to 10 m × 10 m,  
216 and grassland plots 1 m × 1 m to 2 m × 2 m. In forest and shrubland plots, all woody  
217 species were recorded, including species name, growth form, phenological period,  
218 abundance number of individuals or clumps, height, stem diameter, and crown width.  
219 Diameter was generally measured as diameter at breast height (DBH). For individuals  
220 < 2 m tall or when DBH was not applicable, basal diameter (BD) was recorded. In forest  
221 plots, individuals with height ≥ 5 m were assigned to the tree layer, whereas shrubs and  
222 tree seedlings with height < 5 m were classified into the shrub layer. In grassland plots,  
223 all herbaceous species were recorded, including species name, growth form,  
224 phenological period, abundance number of individuals or clumps, maximum leaf-layer  
225 height, and coverage. The number of individuals or clumps was used as the count-based  
226 abundance measure. For species occurring as discrete individuals, each individual was  
227 counted separately. For clumped plants, distinguishable clumps were used as the  
228 counting unit, and the number of individuals within clumps was additionally noted

229 when identifiable. In forest and shrubland plots, woody plants were recorded by  
 230 individual or clump; therefore, the same species could have multiple records within a  
 231 plot. In grassland plots, herbaceous plants were recorded by species, with each species  
 232 represented by one record containing the total number of individuals or clumps within  
 233 the plot.

234 For each plot, longitude, latitude, elevation, community height and total coverage,  
 235 as well as disturbance intensity were recorded. The global position system was used to  
 236 determine the geographic coordinates. Community height was defined as the maximum  
 237 height of the dominant vegetation layer within a plot. Specifically, in forest plots, it  
 238 referred to the visually estimated height of the tallest tree in the tree layer; in shrubland  
 239 plots, it was measured or estimated as the height of the tallest shrub layer using a tape  
 240 measure where possible; and in grassland plots, it was measured as the maximum height  
 241 of the herbaceous leaf layer. Total coverage was ~~and coverage were~~ visually estimated  
 242 in the field as the vertically projected percentage cover of all plant species within each  
 243 plot. Disturbance intensity was assessed directly at four levels: none, weak, medium,  
 244 and strong. These measurements and estimates followed the same field criteria  
 245 throughout all survey campaigns and were conducted by experienced vegetation  
 246 investigators to ensure consistency. In total, 314 plots were surveyed, belonging to 142  
 247 forest plots, 110 shrubland plots, and 62 grassland plots (Fig. 2; Table 1). These  
 248 surveyed plots cover the major geographical space (Fig. 2a), climatic space (Fig. 2b),  
 249 vegetation types (Fig. 2c), and elevational belts (Fig. 2d) of the study region.

250 **Table 1** Summary statistics of plots in the HDM-Plot dataset

Plot	All	Forest	Shrubland	Grassland
Number of plots	314	142	110	62
Longitude (°E)	92.055–104.581	92.661–104.581	92.055–103.941	92.325–103.771
Latitude (°N)	25.547–33.077	25.547–32.749	25.557–33.065	26.423–33.077
Elevation (m)	754–4932	754–4377	1144–4758	3168–4932
SR (species / plot)	1–37 (11 ± 6)	2–37 (13 ± 7)	1–22 (6 ± 4)	3–24 (12 ± 5)

Height (m)	0.001–49.0 (8.238 ± 8.982)	5.2–49.0 (16.0 ± 7.8)	0.1–10.0 (2.8 ± 2.2)	0.001–0.500 (0.081 ± 0.079)
Coverage (%)	10–100 (71 ± 18)	35–100 (71 ± 15)	10–100 (66 ± 20)	15–100 (79 ± 18)
Number of families	117	91	53	38
Number of genera	379	239	124	114
Number of species	1127	737	321	266

251 Values for species richness (SR), community height, and coverage are presented as ranges, with  
 252 mean ± SD in parentheses.

### 253 3.2 Data processing and analysis

254 Species were identified following national and regional floras, including the *Flora*  
 255 *Republicae Popularis Sinicae* (Editorial Committee of Flora of China, Chinese  
 256 Academy of Sciences, 1959–2004), *Flora of Yunnan* (Kunming Institute of Botany,  
 257 Chinese Academy of Sciences, 1977–2006), *Flora Xizangica* (Integrated Scientific  
 258 Expedition to Qinghai-Tibet Plateau, Chinese Academy of Sciences, 1983–1987), and  
 259 *Flora of Sichuan* (Gao et al., 1981). Final species names were then standardized and  
 260 validated against the iPlant online taxonomic system (<http://www.iplant.cn/>, last access:  
 261 16 January 2026). In the most recent taxonomy system of *Flora of Pan-Himalaya*  
 262 (Zhang, 2010), *Kobresia* is classified into *Carex*. Given the ecological importance of  
 263 *Kobresia* in alpine zonal vegetation, and in order to maintain consistency with  
 264 vegetation literatures, we retained *Kobresia* as a traditional genus name for data  
 265 analyses, while the dataset provides both names.

266 Growth forms were classified from field observations following the definitions in  
 267 *Vegetation of China* (Editorial Committee of the Vegetation of China, 1980) into tree,  
 268 shrub, climber, semi-shrub, and herb. Some taxa (e.g., *Quercus* and *Rhododendron*) can  
 269 show both shrubs and small trees, and they were recorded at the plot level according  
 270 to the observed status. For regional summary analyses, each species was additionally  
 271 assigned a single predominant growth form based on its most frequent form seen in the  
 272 field across the dataset. Woody species were further divided by leaf type (needleleaf vs.

273 broadleaf) and phenology (evergreen vs. deciduous). Herbaceous species were  
274 categorized into annual, biennial, and perennial life forms. Floristic areal-types of plant  
275 families and genera were assigned primarily based on the *Areal-types of the World*  
276 *Families and Chinese Genera of Seed Plants* (Wu et al., 1991, 2003), supplemented by  
277 the *Floristic Statistics and Analyses of Seed Plant from China* (Li, 1996) and *Dictionary*  
278 *of the Families and Genera of Chinese Vascular Plants* (iFlora Initiative of Kunming  
279 Institute of Botany, Chinese Academy of Sciences, 2018).

280 Vegetation classification followed the *revised scheme of vegetation classification*  
281 *system of China* (Guo et al., 2020), which adopted a three-level hierarchy (vegetation  
282 formation, alliance, and association) and emphasizes constructive and dominant species  
283 in reflecting the primary structural characteristics of plant communities. For each level,  
284 a corresponding supplementary classification unit was defined (vegetation formation  
285 group, alliance group, and association group). Dominance was identified using species  
286 importance value (IV, %) calculated following Fang et al. (2009): for tree-layer species,  
287 IV combined relative abundance, relative height, and relative basal area; for shrub-layer  
288 species, IV combined relative abundance and relative height; and for herb-layer species,  
289 relative abundance and relative coverage. Relative abundance was calculated from the  
290 number of individuals or clumps, with and all relative metrics were expressed as ~~the~~  
291 percentages of a-the corresponding plot total. A community was assigned a single  
292 dominant species when one species had  $IV > 75\%$ . When multiple species showed IV  
293 between 10% and 75%, species were designated as dominant and sub-dominant in  
294 descending order of IV if interspecific IV differences exceeded 10%, and as co-  
295 dominant when IV differences were  $\leq 10\%$ . When all species had  $IV < 10\%$ , the  
296 community was treated as lacking a clear dominant species, and thereby species were  
297 simply ranked by IV (Wang et al., 2020). Vegetation formation groups were defined by  
298 community ecological physiognomy (e.g., forests), and vegetation formations by the  
299 life form of the constructive species (e.g., evergreen needleleaf forests). Alliance groups  
300 were divided by the genus of constructive species (e.g., *Abies* forest alliance group),  
301 and alliances by the constructive species (e.g., *A. georgei* forest alliance). Association  
302 groups were identified by the constructive species together with the life form of sub-

303 dominant species (e.g., *A. georgei* - shrub forest association group), and associations  
304 were determined by the constructive species and sub-dominant species (*A. georgei* -  
305 *Rubus amabilis* forest association). In the naming convention, a “-” was used to connect  
306 species from different layers, and “+” was to connect multiple species within the same  
307 layer (Guo et al., 2020). In addition, two-way indicator species analysis (TWINSPAN)  
308 was further used as a complementary numerical classification of the vegetation plots. It  
309 is a divisive hierarchical classification method that progressively partitions plots  
310 according to differences in species composition and identifies indicator or diagnostic  
311 species associated with each split.

## 312 **4 Data description**

### 313 **4.1 Species composition**

314 The HDM-Plot dataset compiles 14,113 individual records from 314 plots,  
315 documenting 1,127 plant species (including subspecies and varieties) belonging to 379  
316 genera and 117 families (Table 1). The most ~~species-species-~~rich families are Rosaceae  
317 (133 species), Ericaceae (93), Fabaceae (66), Asteraceae (63), and Fagaceae (37),  
318 occurring in 27.1% to 71.3% of plots (Fig. 3a; Table 2). ~~These families show distinct~~  
319 ~~spatial and elevational patterns (Fig. 3).~~ Rosaceae is the most widely distributed family  
320 in the dataset, while and Fabaceae is also broadly recorded but with a relatively lower  
321 plot frequency. are widespread, whereas Ericaceae and Fagaceae are mainly  
322 concentrated in the southern to central parts, and are less frequent toward the northern  
323 sector. and Asteraceae is more frequently recorded in the central and northern areas, but  
324 is sparse reduced in the southernmost part (Fig. 3a). Along the ~~ranges of~~  
325 ~~elevation~~ elevational range surveyed, Rosaceae and Ericaceae show broad elevational  
326 distributions, with most records concentrated at middle to high elevations. Fabaceae  
327 spans the ~~full-widest~~ elevational ranges, extending from low valleys to alpine areas, but  
328 its distribution is mainly centered at low to middle elevations gradient (750–5000 m).  
329 ~~Rosaceae and Asteraceae extend to the highest elevations but generally occur above~~  
330 ~~1,100 and 1,700 m, respectively.~~ Asteraceae is distinctly concentrated at high elevations,

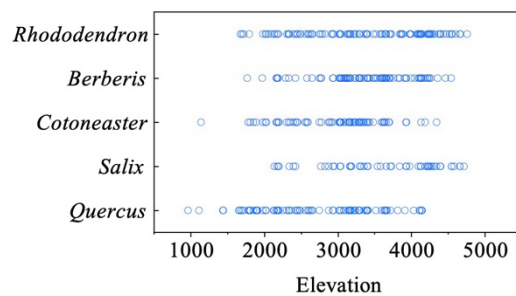
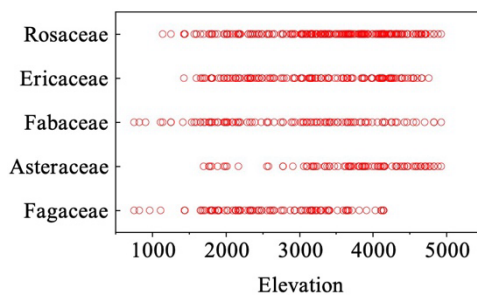
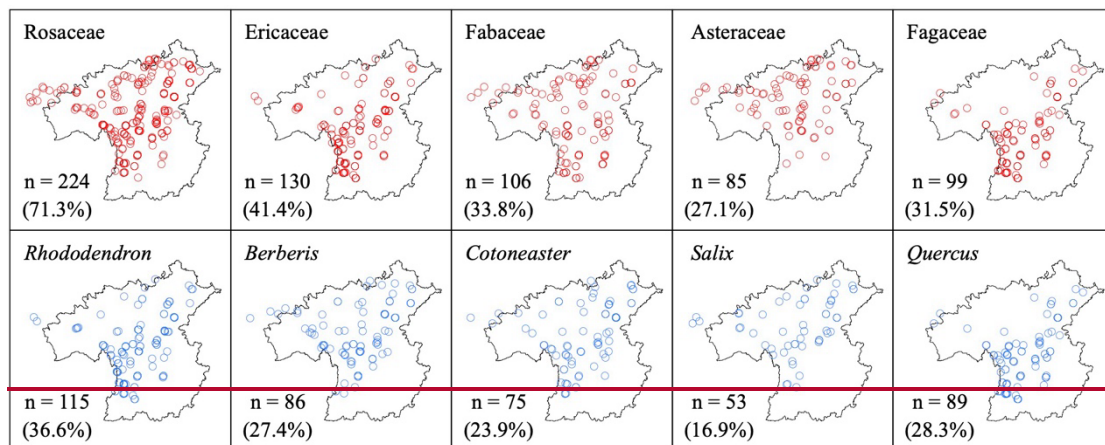
331 ~~with a relatively high median elevation. In contrast, Ericaceae is largely distributed in~~  
332 ~~middle and high elevations (1,400–4,800 m), and Fagaceae is mainly distributed at low~~  
333 ~~to middle elevations and shows a lower elevational distribution center than the other~~  
334 ~~dominant families extends from the lowest elevations up to 4,200 m (Fig. 3c).~~ The five  
335 richest genera ~~were~~ are *Rhododendron* (75 species), *Berberis* (34), *Cotoneaster* (30),  
336 *Salix* (24), and *Quercus* (22) (Table 2). *Rhododendron*, *Berberis*, and *Cotoneaster* are  
337 broadly distributed across the region, although their records are denser in the southern  
338 and central sectors. ~~while~~ *Salix* is more frequent in the northern sector, whereas ~~less in~~  
339 ~~the central to southern HDM and~~ *Quercus* is mainly concentrated in the southern to  
340 central parts and becomes less frequent toward the north (Fig. 3b). ~~The dominant genera~~  
341 ~~occupy wide elevational ranges of approximately 2,600–3,000 m, but their elevational~~  
342 ~~lower and upper limits differ~~ *Rhododendron* and *Berberis* are mainly concentrated at  
343 middle to high elevations, Cotoneaster occupies a relatively broad middle-elevation  
344 range, Salix is centered at higher elevations, and Quercus shows the lowest elevational  
345 distribution center among the dominant genera, mainly occurring at low to middle  
346 elevations (Fig. 3d).

347 **Table 2** Composition of dominant plant families and genera in the HDM-Plot dataset

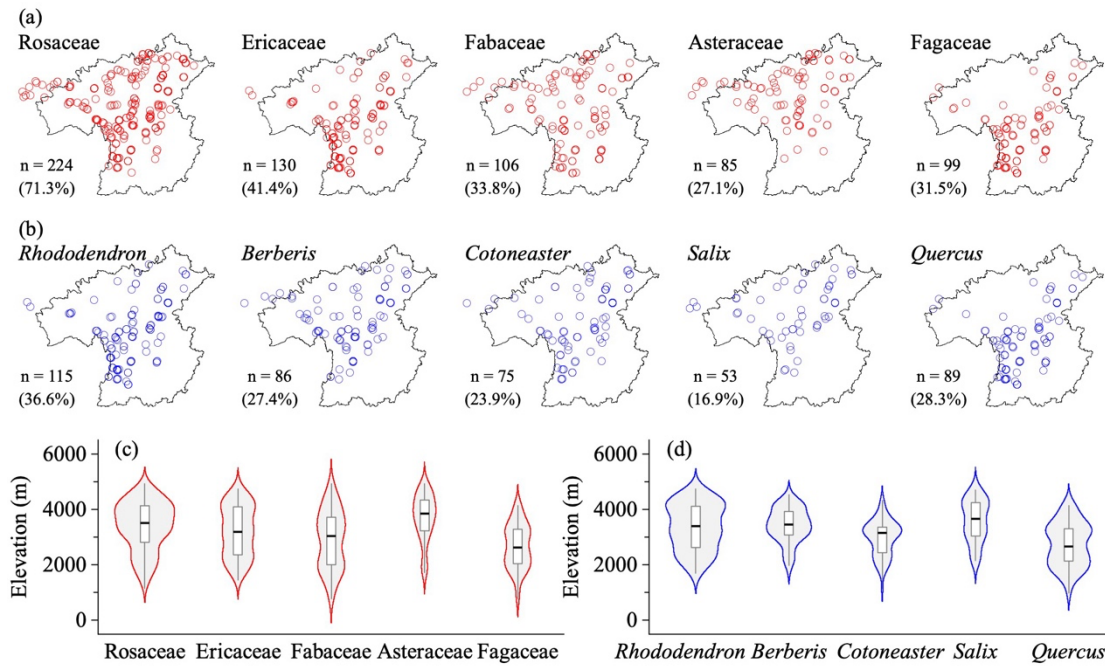
	Dominant families	Dominant genera
All	Rosaceae (133, 11.8%)	<i>Rhododendron</i> (75, 6.7%)
	Ericaceae (93, 8.3%)	<i>Berberis</i> (34, 3.0%)
	Fabaceae (66, 5.9%)	<i>Cotoneaster</i> (30, 2.7%)
	Asteraceae (63, 5.6%)	<i>Salix</i> (24, 2.1%)
	Fagaceae (37, 3.3%)	<i>Quercus</i> (22, 2.0%)
Forest	Rosaceae (99, 13.4%)	<i>Rhododendron</i> (61, 8.3%)
	Ericaceae (78, 10.6%)	<i>Berberis</i> (30, 4.1%)
	Fabaceae & Fagaceae (34, 4.6%)	<i>Cotoneaster</i> (23, 3.1%)
	Berberidaceae (30, 4.1%)	<i>Quercus</i> (20, 2.7%)
	Pinaceae (28, 3.8%)	<i>Salix</i> (19, 2.6%)
Shrubland	Rosaceae (58, 18.1%)	<i>Rhododendron</i> (33, 10.3%)

	Ericaceae (38, 11.8%)	<i>Cotoneaster</i> (19, 5.9%)
	Fabaceae (25, 7.8%)	<i>Berberis</i> (16, 5.0%)
	Berberidaceae (17, 5.3%)	<i>Salix</i> (12, 3.7%)
	Lamiaceae (14, 4.4%)	<i>Lonicera</i> (11, 3.4%)
Grassland	Asteraceae (52, 19.5%)	<i>Gentiana</i> (18, 6.8%)
	Cyperaceae & Ranunculaceae (24, 9.0%)	<i>Kobresia &amp; Saussurea</i> (12, 4.5%)
	Gentianaceae (19, 7.1%)	<i>Anaphalis</i> (10, 3.8%)
	Fabaceae & Rosaceae (18, 6.8%)	<i>Artemisia</i> (9, 3.4%)
	Poaceae (17, 6.4%)	<i>Anemone &amp; Carex</i> (8, 3.0%)

348 Dominant families and genera refer to the top five taxa ranked by number of species. An ampersand  
 349 (&) connects families or genera with the same number of species. The values in parentheses indicate  
 350 the number of species and its proportion of the total number of species in the corresponding category.



351

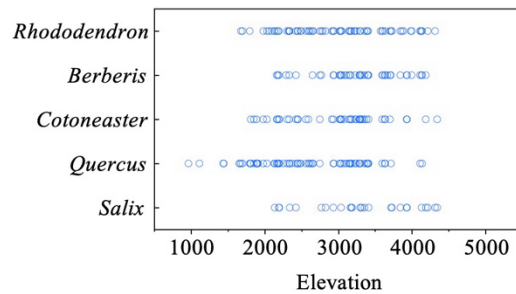
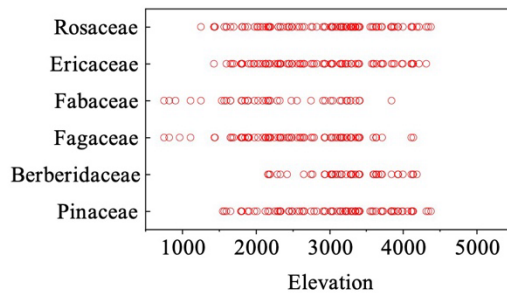
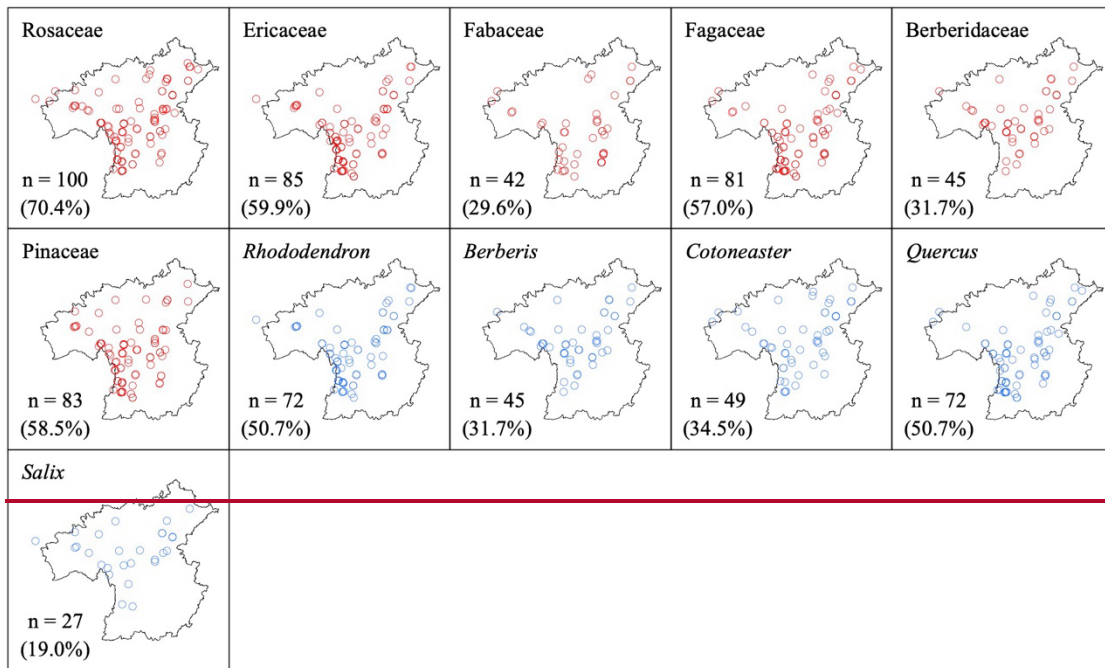


352

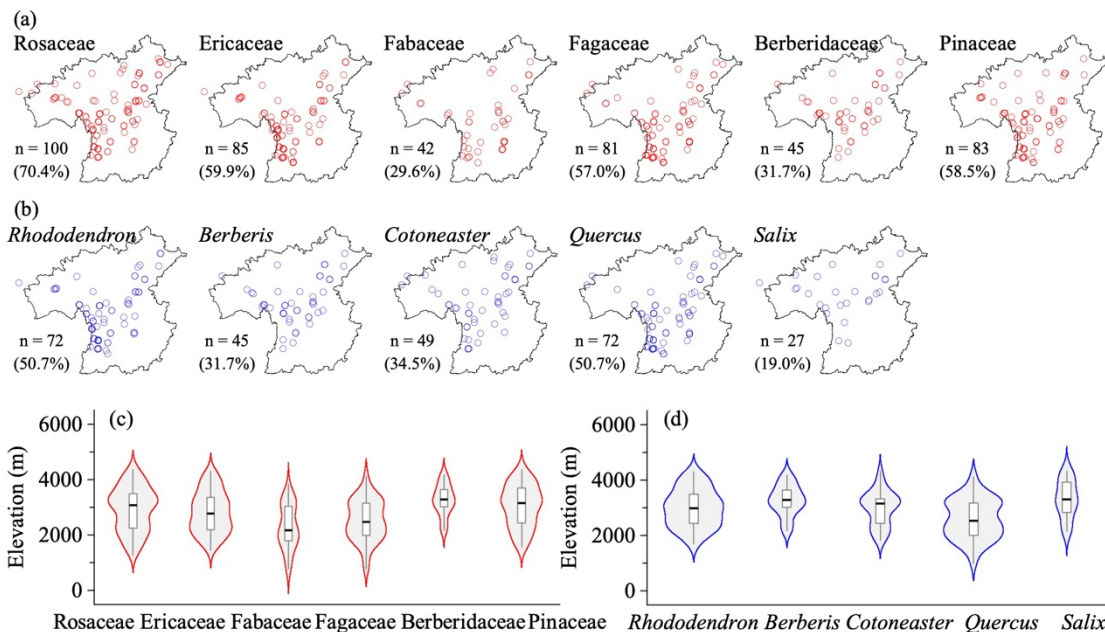
353 **Figure 3.** Horizontal (a, b) and elevational (c, d) Spatial patterns of dominant plant families (a, c)  
 354 and genera (b, d) in all vegetation plots in the HDM-Plot dataset. n denotes the number of plots in  
 355 which each dominant families–family and–or genera–genus were–was recorded, and values in  
 356 parentheses indicate (the proportion of the total number–of survey plots).

357 Taxonomic composition differs among vegetation types (Table 2; Fig. 4–6). Forest  
 358 plots include 737 species, 238 genera, and 91 families (Table 1). The dominant families  
 359 are Rosaceae, Ericaceae, Fabaceae, Fagaceae, Berberidaceae, and PinaceaeSaliceaeae  
 360 (Table 2). Rosaceae is mainly represented by shrub genera such as *Cotoneaster* (23.2%),  
 361 *Rubus* (13.1%), and *Rosa* (12.1%), as well as tree genera such as *Prunus* (14.1%).  
 362 Ericaceae is dominated by *Rhododendron* (78.2%), which is commonly shrubs and  
 363 occasionally small trees. Fabaceae contains a wide range of growth form, including  
 364 shrub genera (e.g., *Indigofera*, *Campylotropis*, and *Caragana*), climbers (mostly single-  
 365 species genera), and occasional tree taxa (e.g., *Dalbergia*). Fagaceae is composed of  
 366 *Quercus* (58.8%), *Lithocarpus* (20.6%), and *Castanopsis* (20.6%), and provides  
 367 constructive species in nearly one-third of forest plots. Berberidaceae only records one  
 368 genus *Berberis* and is a vital component of the shrub layer. Pinaceae offers the main  
 369 needleleaf constructive species in needleleaf forests and mixed forests, dominated by  
 370 *Abies* (35.7%), *Picea* (28.6%), *Larix* (10.7%), and *Pinus* (10.7%). Rosaceae, Ericaceae,  
 371 Fagaceae, Berberidaceae, and Pinaceae are widely recorded in forest plots, whereas

372 Fabaceae and Berberidaceae have lower plot frequencies and more restricted spatial  
373 distributions (Fig. 4a). Rosaceae and Pinaceae occur across a broad part of the region,  
374 while Ericaceae, Fabaceae, Fagaceae, and Berberidaceae are more concentrated in the  
375 southern to central sectors. ~~are the most widely distributed families, and other four~~  
376 ~~dominant families are concentrated in the southern HDM~~ (Fig. 4a). Along the  
377 elevational gradient, Fabaceae and Fagaceae are mainly distributed at low to middle  
378 elevations, although both extend upward into middle-high elevational belts. ~~show the~~  
379 ~~lowest elevational lower limits, with upper limits close to 3,800 m and 4,100 m,~~  
380 ~~respectively.~~ Rosaceae, and Ericaceae, show broad middle-elevation distributions. ~~and~~  
381 ~~Pinaceae reach the highest upper limits (4,300 m), with lower limits between 1,300 and~~  
382 ~~1,500 m.~~ Berberidaceae and Pinaceae have higher elevational distribution centers, with  
383 records mainly concentrated at middle to high elevations ~~exhibits the narrowest~~  
384 ~~elevational range (2,200–4,200 m~~ Fig. 4c). The top five genera are *Rhododendron*,  
385 *Berberis*, *Cotoneaster*, *Quercus*, and *Salix* (Table 2). *Rhododendron*, *Berberis*,  
386 *Cotoneaster*, and *Quercus* ~~The first four genera are restricted to~~ mainly recorded in the  
387 southern HDM to central parts of the study region, while ~~whereas~~ *Salix* is more  
388 frequently recorded in toward the northern HDM sector (Fig. 4b). ~~The upper elevational~~  
389 ~~limits of these genera are similar (4,100–4,300 m), whereas their lower limits differ.~~  
390 *Quercus* ~~occurs down to 1,000 m~~ has the lowest elevational distribution center and is  
391 mainly concentrated at low to middle elevations, *Rhododendron* to 1,700 m, and  
392 *Cotoneaster* occupy broad middle-elevation range. ~~to 1,800 m, and *Berberis* is more~~  
393 narrowly concentrated at middle to high elevations, ~~and while *Salix* to approximately~~  
394 2,100 m ~~is centered at relatively high elevations among the dominant forest genera~~ (Fig.  
395 4d).



396

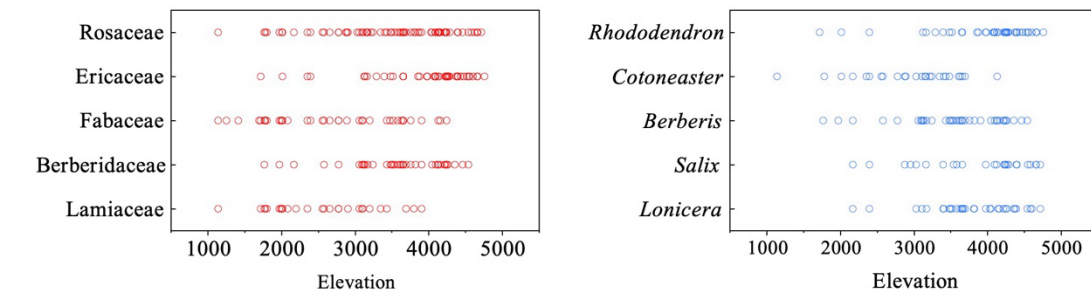
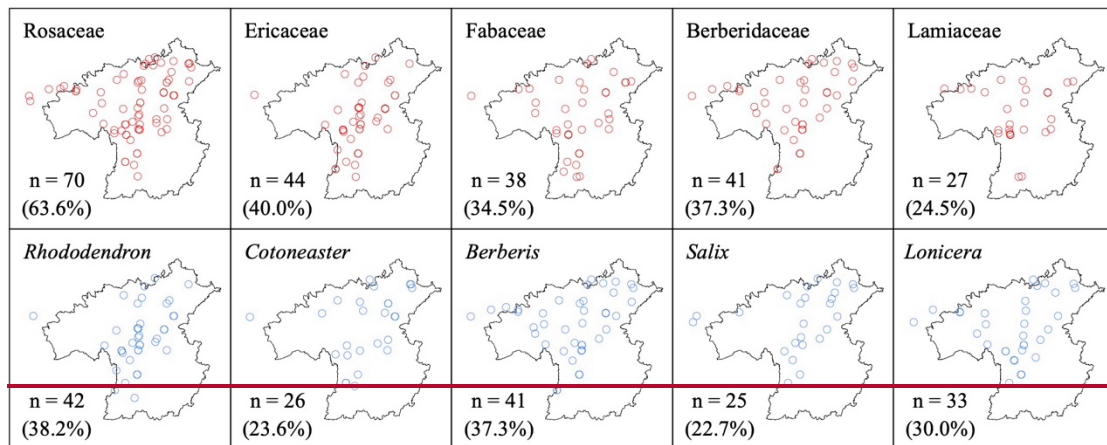


397

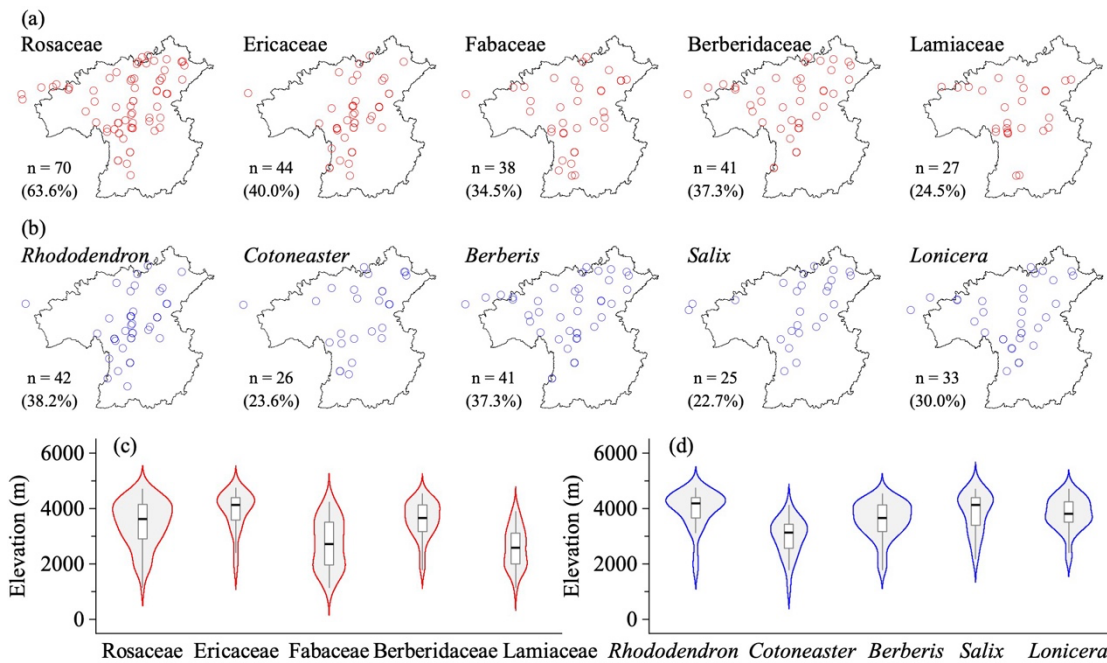
398 **Figure 4. Horizontal (a, b) and elevational (c, d) Spatial patterns of dominant plant families (a, c)**  
399 **and genera (b, d) in forest vegetation plots in the HDM-Plot dataset. n denotes the number of plots**  
400 **in which each dominant family or genus was recorded, and the values in parentheses indicate the**  
401 **proportion of all forest plots.**

402 110 shrubland plots survey a total of 321 species from 124 genera and 53 families  
403 (Table 1). Dominant families largely overlap with those of forests, with Lamiaceae as a  
404 new component. Rosaceae consists of *Cotoneaster* (32.8%), *Rosa* (15.5%), and *Spiraea*  
405 (13.8%) and forms the core of deciduous broadleaf shrublands. Ericaceae is strongly  
406 dominated by *Rhododendron* (86.8%) and typically acts as the constructive species in  
407 evergreen broadleaf shrublands. Fabaceae includes *Caragana* (20.0%), *Campylotropis*  
408 (16.0%), and *Indigofera* (16.0%), commonly recorded in the dry-hot valley shrublands.  
409 Berberidaceae is almost represented by *Berberis* (94.1%), with *Mahonia* recorded but  
410 not in forest plots. Lamiaceae is characterized by typical dry-hot valley genera such as  
411 *Caryopteris* (28.6%), *Isodon* (21.4%), and *Elsholtzia* (21.4%). Rosaceae is the most  
412 widely distributed shrubland family across the study region, whereas ~~and~~ Fabaceae and  
413 Berberidaceae are widespread and also broadly recorded, ~~whereas Berberidaceae,~~  
414 Ericaceae is more concentrated in the southern to northwestern sectors, and Lamiaceae  
415 are ~~heterogeneous in distribution~~ mainly distributed in the north (Fig. 5a). Ericaceae has  
416 the highest elevational distribution center and is mainly concentrated in high elevations,  
417 and Berberidaceae is also mainly distributed at middle to high elevations. Rosaceae  
418 spans a broad elevational range but is denser at middle to high elevations, while  
419 Fabaceae and Lamiaceae have lower elevational distribution centers and are mainly  
420 concentrated at low to middle elevations ~~Shrubland composition transitions from lower-~~  
421 ~~elevational dry-hot valley components to middle and high elevations with increased~~  
422 ~~representation of Ericaceae and Berberidaceae~~ (Fig. 5c). The top genera are  
423 *Rhododendron*, *Cotoneaster*, *Berberis*, *Salix*, and *Lonicera* (Table 2). *Berberis* and  
424 *Lonicera* are widely distributed across the region, whereas *Rhododendron*, *Cotoneaster*,  
425 and *Salix* are primarily aligned along a southwest–northeast direction (Fig. 5b). Their  
426 elevational distributions are also distinct. *Rhododendron* and *Salix* are concentrated at  
427 high elevations, with higher median elevations and relatively narrow central  
428 distributions. *Berberis* and *Lonicera* are mainly distributed at middle to high elevations.  
429 *Cotoneaster* has a lower elevational distribution center, and is mainly concentrated at  
430 middle elevations ~~Although these genera occasionally occur at low elevations, they are~~  
431 ~~largely distributed between 3,000 and 4,700 m, with *Cotoneaster* having the lowest~~

432 upper limit (3,700 m) (Fig. 5d).



433



434

435 **Figure 5.** Horizontal (a, b) and elevational (c, d) spatial patterns of dominant plant families (a, c)  
 436 and genera (b, d) in shrubland vegetation plots in the HDM-Plot dataset. n denotes the number of  
 437 plots in which each dominant family or genus was recorded, and the values in parentheses indicate  
 438 the proportion of all shrubland plots.

439

62 grassland plots investigate a total of 266 species belonging to 38 families and

440 113 genera (Table 1). The most species-rich families are Asteraceae, Cyperaceae,  
441 Ranunculaceae, Gentianaceae, Fabaceae, Rosaceae, and Poaceae (Table 2). Asteraceae  
442 is largely represented by *Saussurea* (23.1%), *Anaphalis* (19.2%), *Artemisia* (17.3%),  
443 and *Taraxacum* (13.5%), consisting of perennial forbs and semi-shrubs that contribute  
444 to forb grasslands. Cyperaceae is dominated by tussock *Kobresia* and rhizome *Carex*  
445 and provide the main constructive species in grassland vegetation (42 plots), especially  
446 the zonal species *K. pygmaea*. Ranunculaceae is represented by *Anemone* (33.3%) and  
447 *Ranunculus* (20.8%), Gentianaceae is strongly dominated by *Gentiana* (94.7%), and  
448 Fabaceae is composed of *Astragalus* (33.3%) and *Oxytropis* (27.8%). Rosaceae consists  
449 of perennial herbs such as *Argentina* (33.3%) and *Potentilla* (22.2%) and dwarf shrub  
450 *Dasiphora* (11.1%). Poaceae is dominated by tussock grasses, including *Poa* (17.6%),  
451 *Aristida* (17.6%), *Stipa* (11.8%), and *Festuca* (11.8%). The dominant grassland families  
452 are mainly distributed in the central and northern parts of the HDM-Plot study region  
453 (Fig. 6a). Asteraceae, Cyperaceae, Ranunculaceae, Rosaceae, and Poaceae are broadly  
454 recorded across grassland plots, whereas Gentianaceae and Fabaceae have relatively  
455 lower plot frequencies (Fig. 6a). Their elevational distributions are concentrated in  
456 high-elevation belts, but with slight differences in distribution centers and ranges (Fig.  
457 6c). ~~Grassland families show broadly similar distributions across the surveyed region~~  
458 (~~Fig. 6~~). The dominant genera include *Gentiana*, *Kobresia*, *Saussurea*, *Anaphalis*,  
459 *Artemisia*, *Anemone*, and *Carex* (Table 2). *Kobresia* is the most broadly distributed  
460 dominant grassland genus across both horizontal space and the elevational gradient,  
461 consistent with its role as a major alpine meadow constructive genus ~~shows the broad~~  
462 distribution across both geographic space and the elevational gradient, whereas the  
463 other dominant genera exhibit distinct differentiation along both dimensions (Fig. 6b,  
464 d). *Gentiana*, *Saussurea*, *Anaphalis*, *Anemone*, and *Carex* are also mainly concentrated  
465 in high-elevation grasslands, whereas *Artemisia* shows a relatively narrower and  
466 slightly lower elevational distribution compared with the other dominant genera (Fig.  
467 6d).

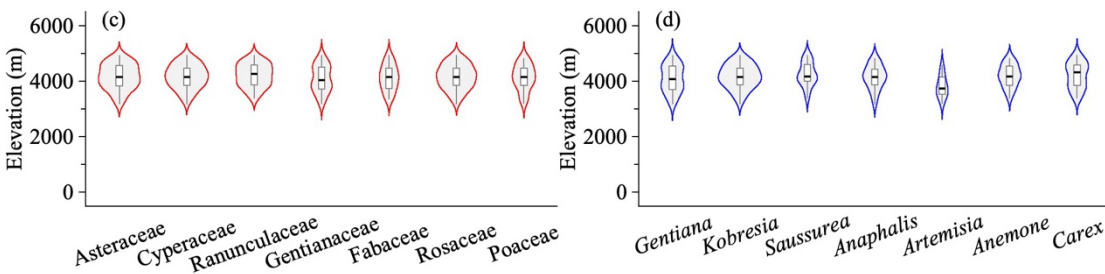
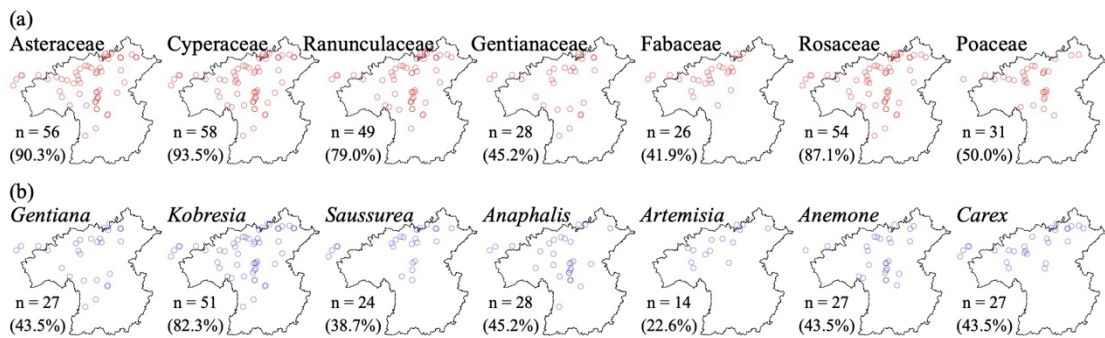
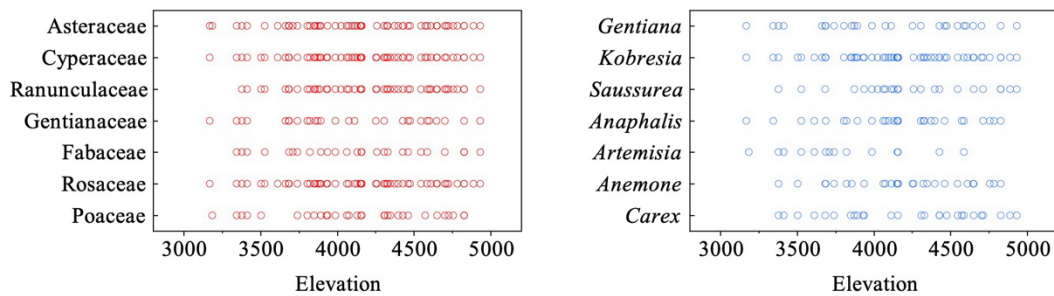
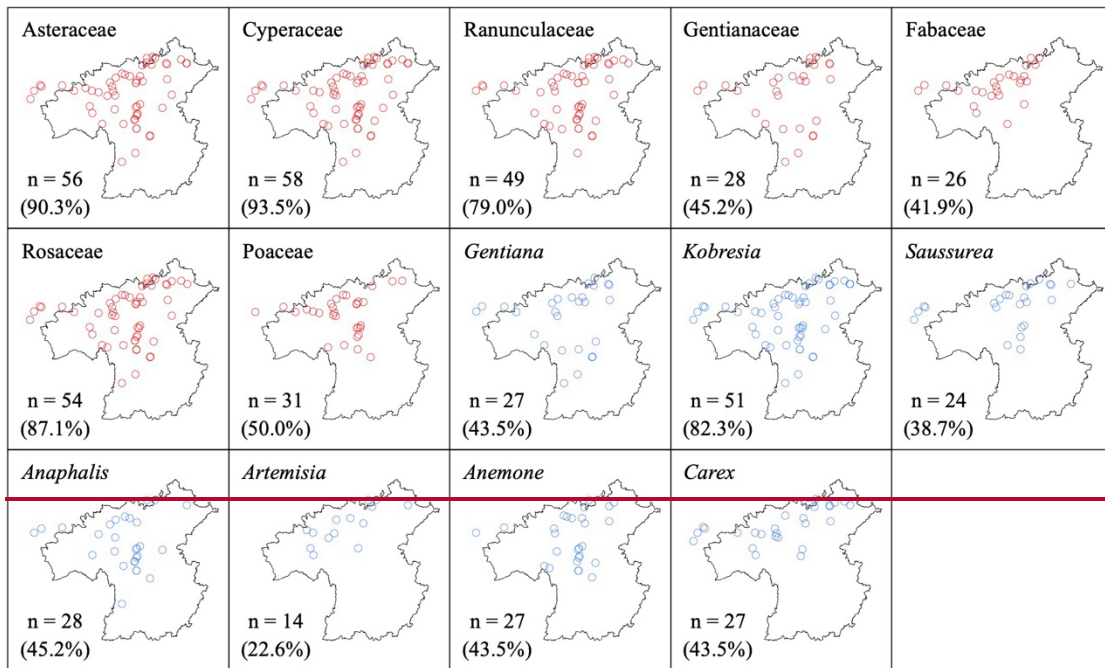
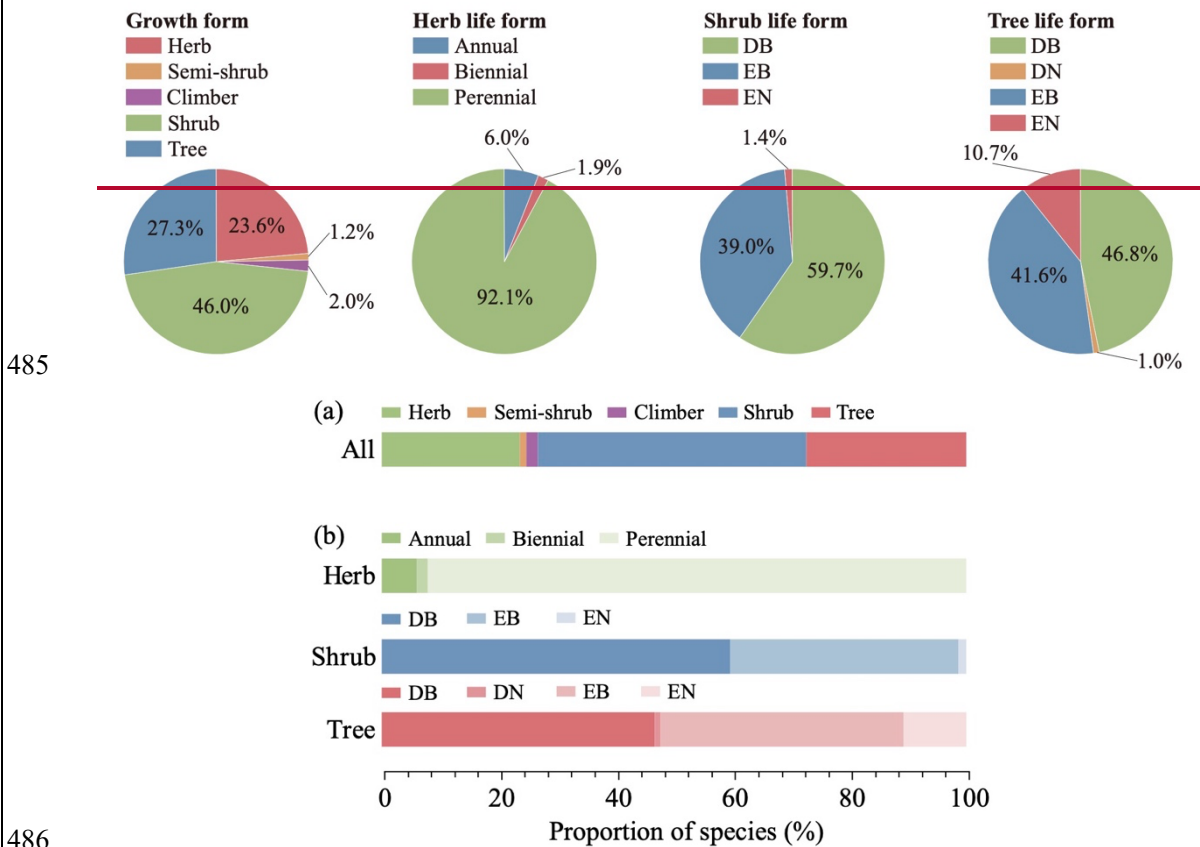


**Figure 6.** Horizontal (a, b) and elevational (c, d) Spatial patterns of dominant plant families (a, c) and genera (b, d) in grassland vegetation plots in the HDM-Plot dataset. n denotes the number of plots in which each dominant family or genus was recorded, and the values in parentheses indicate the proportion of all grassland plots.

474 **4.2 Growth forms and life forms**

475 The 1,127 species in the HDM-Plot dataset can be categorized into five growth forms  
 476 (Fig. 7a). Shrubs comprise the largest proportion of recorded species (46.0%), followed  
 477 by trees (27.3%) and herbs (23.6%), while climbers (2.0%) and semi-shrubs (1.2%)  
 478 contribute a small number of species (Fig. 7a). Among herbs, perennials dominate  
 479 (92.1%), ~~and while~~ annuals (6.0%) and biennials (1.9%) are comparatively rare (Fig.  
 480 7b). Woody species show clear contrasts in leaf type and phenology (Fig. 7b). Shrubs  
 481 are almost composed of broadleaf (98.7%), with deciduous shrubs (59.7%) more  
 482 frequent than evergreen shrubs (40.4%), whereas trees exhibit a higher proportion of  
 483 needleleaf species (11.7%) and a near balance between evergreen (52.3%) and  
 484 deciduous (47.8%) species (Fig. 7b).

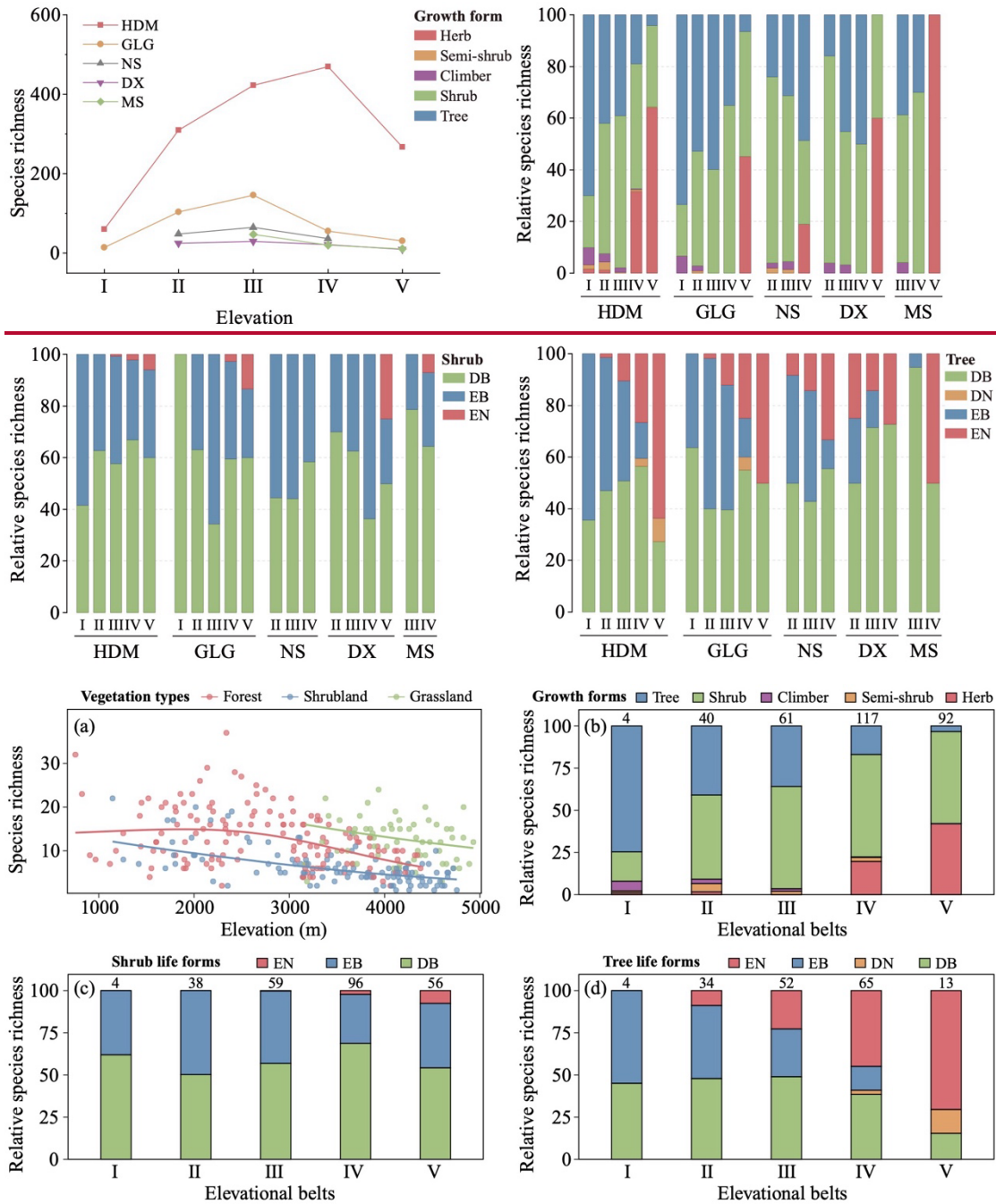


485  
 486  
 487 **Figure 7.** ~~Growth-forms~~Growth-form composition of all species (a) and life-formslife-form  
 488 composition within herbaceous, shrub, and tree species (b)~~of plant species~~ surveyed in the HDM-  
 489 Plot dataset. Bars show the proportion of species in each category. DB, deciduous broadleaf; DN,  
 490 deciduous needleleaf; EB, evergreen broadleaf; and EN, evergreen needleleaf. Pie charts show life  
 491 form classifications for dominant herbs, shrubs, and trees only, and detailed life form information  
 492 for all species is provided in the species list of the published dataset.

493 ~~Pooled~~ In the HDM-Plot study region, plot-level species richness shows distinct  
494 elevational trends among vegetation types after accounting for plot area along the  
495 elevational gradient shows a unimodal pattern at the regional scale (Fig. 8a). Forest  
496 plots maintain relatively high species richness from low to middle elevations, followed  
497 by a decline toward higher elevations. Shrubland plots show a decreasing trend along  
498 the elevational gradient. Grassland plots are restricted to middle- and high-elevation  
499 belts, with relatively high richness at the lower part of their observed elevational range  
500 and a gradual decline toward higher elevations, increasing from low elevations to a  
501 maximum at 3,000–4,000 m and then declining sharply. Four individual mountains with  
502 broad elevational coverage (Gaoligong Mt; Nushan Mt; Daxue Mt; and Minshan Mt;  
503 Fig. 2) show similar unimodal patterns, although peak richness occurs at 2,000–3,000  
504 m in these mountains (Fig. 8).

505 ~~Growth~~ Growth-form composition varies significantly with elevation clearly  
506 across elevational belts in surveyed plots (Fig. 8b). The relative contribution of trees is  
507 highest ~~Trees dominate at the lowest elevations~~ elevational belt and declines with  
508 increasing elevation, shrubs ~~Shrubs remain the major component from low-middle to~~  
509 high elevations and are especially prominent in the middle-elevation belts. important  
510 across all belts and peak at middle elevations (2,000–3,000 m), and h ~~Herbs increase~~  
511 strongly toward the highest elevations ~~elevational belt. Woody life-life-form~~  
512 composition also shifts with elevation (Fig. 8c, d). For shrubs, evergreen broadleaf  
513 shrubs are most frequent in low elevations (0–1,000 m), deciduous broadleaf shrubs  
514 dominate from middle to high elevations (1,000–5,000 m) most elevational belts,  
515 whereas evergreen broadleaf shrubs contribute substantially across the elevational  
516 gradient, particularly from low to middle elevations. and e ~~Evergreen needleleaf shrubs~~  
517 are absent or rare at lower elevations and occur mainly above 2,000 m in the upper  
518 elevational belts (Fig. 8c). Tree Life-life forms composition of trees shows more  
519 significant stronger elevational shiftsturnover (Fig. 8d). Evergreen broadleaf trees are  
520 more common at low elevations but and decrease with elevations sharply toward higher  
521 elevations, d ~~Deciduous broadleaf trees contribute substantially from low to middle-~~  
522 high elevations but increase to middle elevations and then decline in the highest belt. ;

523 ~~e~~Evergreen needleleaf trees ~~rise rapidly above 1,000 m~~increase with elevation and  
 524 ~~dominate at high elevations,~~become dominant in the upper belts. and ~~d~~Deciduous  
 525 needleleaf trees are largely restricted to ~~the high-elevation~~belts (3,000–5,000 m)(Fig.  
 526 8d). ~~At the mountain scale, several elevational trends are consistent with the regional~~  
 527 ~~pattern, but changes specific to individual mountains are also evident and unique (Fig.~~  
 528 ~~8).~~



529

530

531 **Figure 8.** ~~Changes in~~Elevational patterns of plot-level species richness ~~(a) of,~~ growth forms ~~(b),~~ and  
 532 ~~woody life forms~~ ~~(c, d)~~ along elevational gradients in the HDM-Plot dataset. ~~In panel (a), points~~

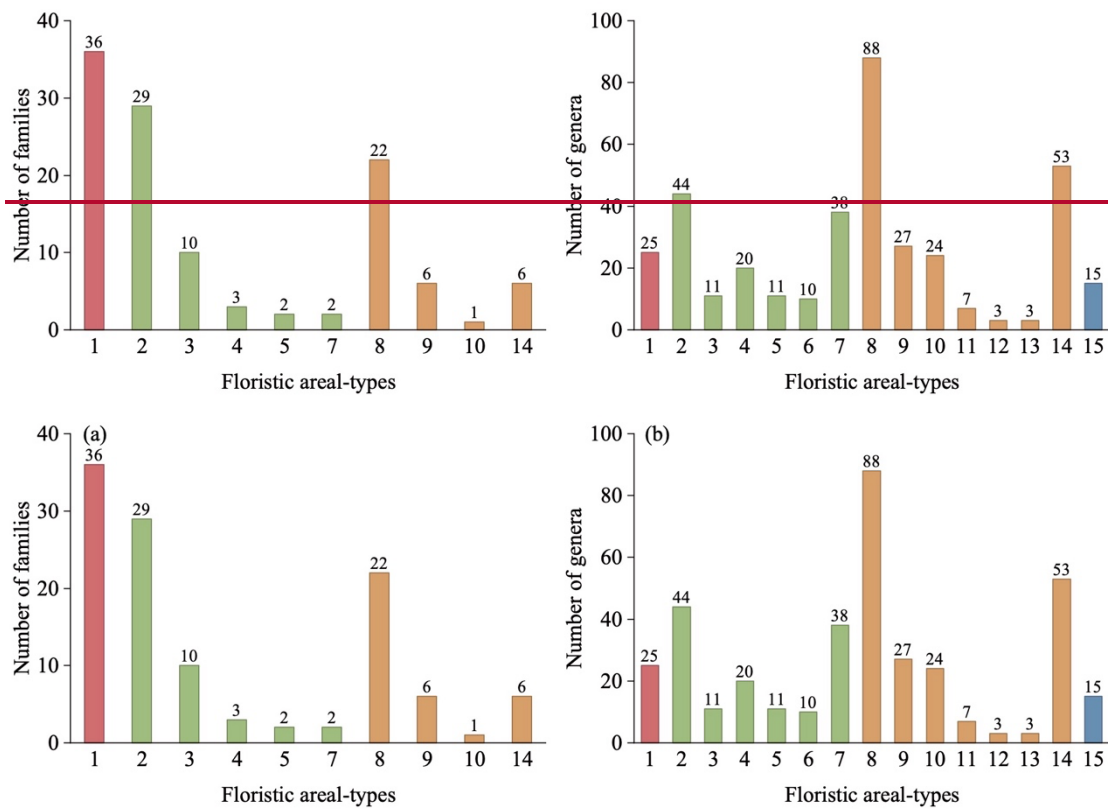
533 represent observed species richness in individual plots, and fitted lines show elevational trends  
534 estimated using generalized additive models with plot area included as a covariate. Predictions were  
535 standardized to representative plot areas of 100 m<sup>2</sup> for forests, 25 m<sup>2</sup> for shrublands, and 1 m<sup>2</sup> for  
536 grasslands. Panels (b–d) show mean plot-level proportions within each elevational belt. Elevational  
537 patterns are summarized at two scales. Regional scale (HDM, Hengduan Mountains): species  
538 richness represents the combined number of unique species with each elevational belt across the  
539 entire study area. Elevational belts are defined as I, 0–1000 m; II, 1000–2000 m; III, 2000–3000 m;  
540 IV, 3000–4000 m; and V, 4000–5000 m. n denotes the number of plots included in each elevational  
541 belt. Local scale: four representative mountains with extensive elevational gradients distributed  
542 from south to north within the dataset are selected. GLG, Gaoligong Mountain; NS, Nushan  
543 Mountain; DX, Daxue Mountain; and MS, Minshan Mountain. The abbreviations of woody life  
544 forms are defined as follows: DB, deciduous broadleaf; DN, deciduous needleleaf; EB, evergreen  
545 broadleaf; and EN, evergreen needleleaf.

### 546 4.3 Floristic characteristics

547 At the family level, 117 families can be assigned to 10 areal-type categories (Fig.  
548 9a). Cosmopolitan families account for 30.8% of the total, tropical families for 39.3%,  
549 and temperate families for 29.9%. Pantropic families comprise the largest share within  
550 tropical families (63.0%), with species-rich families including Lauraceae, Sapindaceae,  
551 Celastraceae, Euphorbiaceae, and Anacardiaceae. North temperate families account for  
552 62.9% of the temperate component, represented by Ericaceae, Fagaceae, Berberidaceae,  
553 Salicaceae, and Pinaceae. These patterns reflect that the floristic composition of the  
554 HDM-Plot study region retains a tropical–subtropical elements and also incorporating  
555 temperate–alpine attributes.

556 At the genus level, 379 genera can be assigned into 15 areal-type categories (Fig.  
557 9b). Temperate genera dominate (54.1%), followed by tropical genera (35.4%), whereas  
558 cosmopolitan (6.6%) and Chinese endemic genera (4.0%) are less frequent. Temperate  
559 genera are mainly north temperate (42.9%), represented by *Rhododendron*, *Berberis*,  
560 *Cotoneaster*, *Salix*, and *Quercus*. For tropical genera, pantropical (32.8%) and tropical  
561 Asian (28.4%) areal-types are most common, with *Ilex* and *Indigofera* as pantropical  
562 representatives and *Fargesia*, *Leptodermis*, *Caryopteris*, and *Corylopsis* as East Asian  
563 representatives. Compared with the family level, the genus level composition shows a  
564 clear shift toward temperate elements. However, when the number of species contained  
565 in each areal-type group is considered, temperate genera account for 66.7% of the

566 recorded species, whereas tropical genera account for 23.3% (Table S2). A plot–genus  
 567 occurrence analysis further shows that temperate genera dominate plot-level occurrence  
 568 records and are mainly associated with high elevations, whereas tropical genera are  
 569 more closely associated with low elevations (Fig. S2). Both temperate and tropical  
 570 genera are spatially widespread within the study region, but the number of plot-level  
 571 occurrence records of temperate genera is nearly four times that of tropical genera (Fig.  
 572 S2). Therefore, the dataset records transitional floristic features across the Hengduan  
 573 Mountains and adjacent regions, while temperate elements remain dominant when  
 574 species representation and plot-level occurrence are considered.



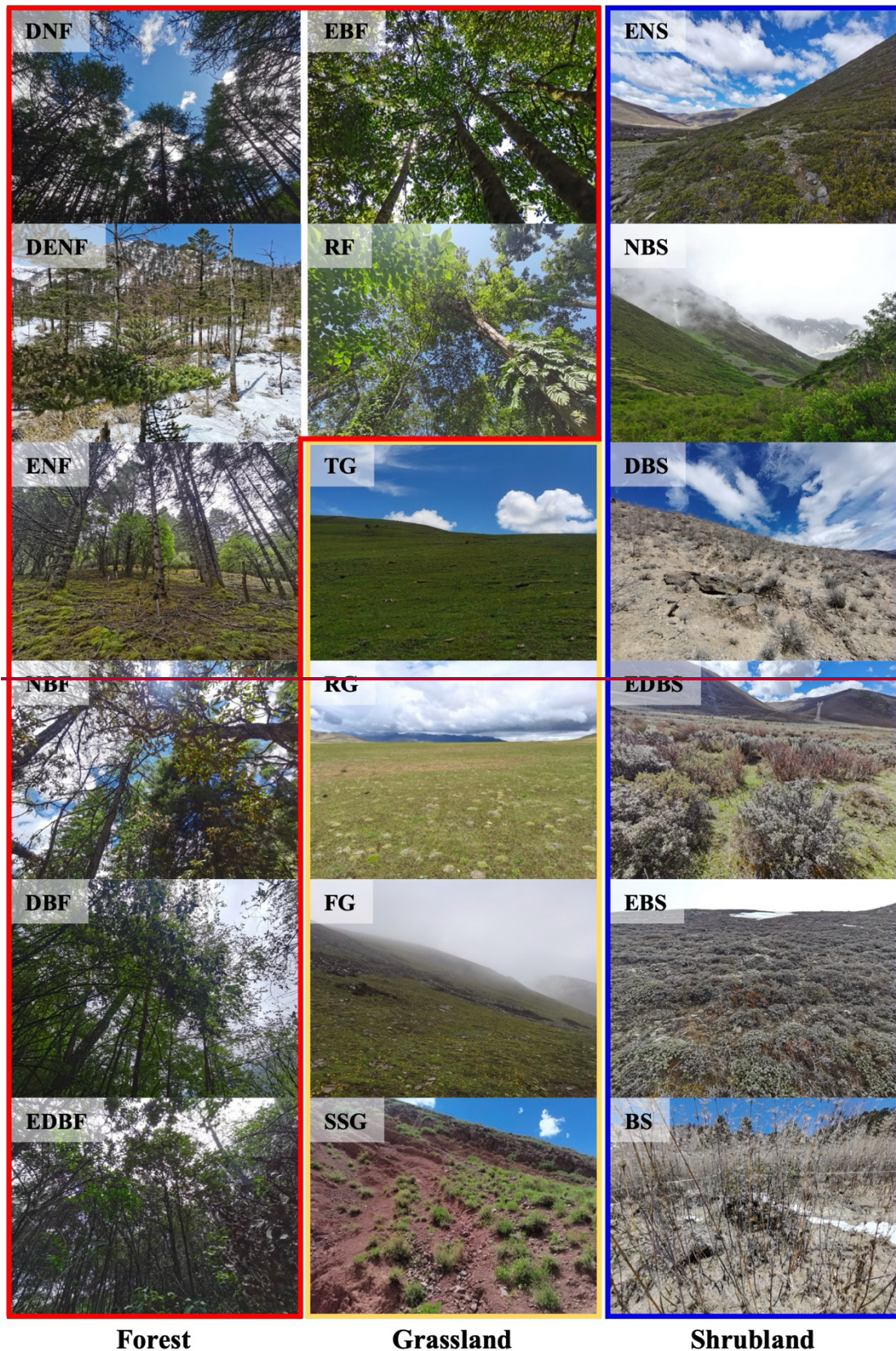
575

576

577 **Figure 9.** Floristic areal-types of plant families **(a)** and genera **(b)** surveyed in the HDM-Plot dataset.  
 578 1, Cosmopolitan; 2, Pantropic; 3, Tropical Asia & Tropical America disjunct; 4, Old World  
 579 Tropics; 5, Tropical Asia & Tropical Australasia; 6, Tropical Asia to Tropical Africa; 7, Tropical  
 580 Asia (Indo–Malaysia); 8, North Temperate; 9, East Asia & North America disjunct; 10, Old World  
 581 Temperate-; 11, Temperate Asia; 12, Mediterranean, West Asia to Central Asia; 13, Central Asia; 14,  
 582 East Asia; and 15, Endemic to China (Wu, 1991, 1993–2003). Bar colors indicate four floristic areal-  
 583 type groups: cosmopolitan (red), tropical (green), temperate (orange), and endemic to China  
 584 (blue). The green and orange bars represent tropical and temperate areal-types, respectively, whereas  
 585 the red and blue bars reflect cosmopolitan and endemic to China areal-types, respectively.

#### 586 4.4 Vegetation classification

587 Based on field surveys and the *revised vegetation classification system of China*  
588 (Guo et al., 2020), 314 plots can be classified into three vegetation formation groups,  
589 namely forest, shrubland, and grassland (Fig. 10–11; Table 3S4). These plots can be  
590 further classified into 18 vegetation formations, 142 alliance groups, 209 alliances, 238  
591 association groups, and 299 associations (Table S4). Because these lower-level units  
592 are highly detailed and many are represented by only one plot, the full hierarchical  
593 classification is provided in Table S4 and in the published dataset, whereas the main  
594 text focuses on vegetation formation groups and vegetation formations (Fig. 10; Table  
595 3).



596  
597  
598  
599  
600

**Figure 10.** Plot photos across 18 vegetation formations in the HDM Plot dataset. DNF, deciduous needleleaf forest; DENF, mixed deciduous and evergreen needleleaf forest; ENF, evergreen needleleaf forest; NBF, mixed needleleaf and broadleaf forest; DBF, deciduous broadleaf forest; EDBF, mixed evergreen and deciduous broadleaf forest; EBF, evergreen broadleaf forest; RF,

601 rainforest; ENS, evergreen needleleaf shrubland; NBS, needleleaf and broadleaf shrubland; DBS,  
 602 deciduous broadleaf shrubland; EDBS, evergreen and deciduous broadleaf shrubland; EBS,  
 603 evergreen broadleaf shrubland; BS, bamboo shrubland; TG, tussock grassland; RG, rhizome  
 604 grassland; FG, forb grassland; SSG, semi shrubby grassland.

605 **Table 3** Vegetation classification of plant communities in the HDM Plot dataset

Vegetation- formation group	Vegetation- formation	Alliance group	Number of- Plot		
Forest	DNF	<i>Larix</i>	4		
	DENF	<i>Larix + Abies</i>	1		
	ENF	<i>Abies</i>	12		
		<i>Cunninghamia</i>	1		
		<i>Juniperus</i>	3		
		<i>Picea</i>	8		
		<i>Picea + Juniperus</i>	1		
		<i>Pinus</i>	21		
		<i>Tsuga</i>	3		
		<i>Tsuga + Abies</i>	1		
	NBF		<i>Abies + Quercus</i>	3	
			<i>Abies + Rhododendron</i>	1	
			<i>Abies + Sorbus</i>	1	
			<i>Acer + Cephalotaxus</i>	1	
			<i>Juniperus + Salix</i>	1	
			<i>Picea + Betula</i>	1	
			<i>Picea + Quercus</i>	1	
			<i>Pinus + Alnus</i>	3	
			<i>Pinus + Castanopsis</i>	1	
			<i>Pinus + Lithocarpus</i>	2	
			<i>Pinus + Populus</i>	1	
			<i>Pinus + Quercus</i>	2	
			<i>Taxus + Acer</i>	1	
			<i>Tsuga + Lithocarpus</i>	1	
		DBF		<i>Alnus</i>	6
				<i>Alnus + Quercus</i>	1
				<i>Betula</i>	5
			<i>Dalbergia</i>	1	
			<i>Populus</i>	3	
			<i>Populus + Litsea + Viburnum</i>	1	
			<i>Prunus</i>	2	
			<i>Pyrus</i>	1	
			<i>Quercus</i>	3	
			<i>Salix</i>	2	
	<i>Tilia + Cornus + Corylus</i>	1			
	<i>Toxicodendron + Quercus</i>	1			

Shrubland	EDBF	<i>Alnus + Castanopsis</i>	†	
		<i>Alnus + Saurauia</i>	†	
		<i>Alnus + Ternstroemia</i>	†	
		<i>Betula + Quercus</i>	†	
		<i>Castanopsis + Litsea</i>	†	
		<i>Castanopsis + Quercus</i>	†	
		<i>Pistacia + Dalbergia</i>	†	
		<i>Quercus + Albizia</i>	†	
		<i>Quercus + Corylopsis</i>	†	
		<i>Quercus + Pistacia</i>	†	
		<i>Salix + Quercus</i>	†	
		EBF	<i>Acacia</i>	†
			<i>Castanopsis</i>	†
	<i>Exbucklandia + Schima</i>		†	
	<i>Lithocarpus</i>		†	
	<i>Lithocarpus + Quercus + Symplocos</i>		†	
	<i>Mallotus + Ficus</i>		†	
	<i>Mallotus + Machilus</i>		†	
	<i>Morella</i>		†	
	<i>Pistacia</i>		2	
	<i>Quercus</i>		12	
	<i>Quercus + Ilex</i>		†	
	<i>Sarcosperma</i>		†	
	<i>Saurauia</i>		†	
	<i>Schima</i>		†	
	RF	<i>Aidia + Oreoenide</i>	†	
		<i>Altingia</i>	†	
		<i>Castanopsis + Altingia</i>	†	
	ENS	<i>Juniperus</i>	10	
		<i>NBS</i>		
	DBS	<i>Juniperus + Ribes + Spiraea</i>	†	
		<i>Salix + Juniperus</i>	†	
		<i>Sibiraea + Juniperus + Caragana</i>	†	
		<i>Abelia + Berberis + Rosa + Cotinus</i>	†	
		<i>Ajania</i>	†	
		<i>Artemisia</i>	†	
		<i>Berberis</i>	6	
		<i>Berberis + Cotoneaster</i>	†	
		<i>Berberis + Lonicera</i>	†	
		<i>Caryopteris</i>	2	
		<i>Corylus</i>	†	
		<i>Cotoneaster – Artemisia</i>	†	
		<i>Elsholtzia + Rubus + Hypericum + Viburnum</i>	†	
		<i>Excoccaria</i>	†	
		<i>Lonicera + Cotoneaster</i>	†	

		<i>Prunus + Zanthoxylum + Isodon</i>	1
		<i>Rhamnus</i>	2
		<i>Rosa</i>	2
		<i>Rosa + Berberis + Isodon</i>	1
		<i>Rosa + Cotoneaster + Berberis</i>	1
		<i>Salix</i>	7
		<i>Salix + Dasiphora</i>	1
		<i>Sibiraea</i>	2
		<i>Sibiraea + Salix</i>	1
		<i>Sophora</i>	1
		<i>Sophora + Bauhinia</i>	1
		<i>Sophora + Leptodermis</i>	1
		<i>Spiraea</i>	1
		<i>Vitex</i>	1
	EDBS	<i>Ajania + Daphne</i>	1
		<i>Campylotropis + Daphne</i>	1
		<i>Dasiphora + Rhododendron</i>	1
		<i>Flueggea + Clematis</i>	1
		<i>Isodon + Rosa</i>	1
		<i>Itea + Viburnum + Bauhinia</i>	1
		<i>Prinsepia + Rosa</i>	1
		<i>Quercus + Olea + Pistacia + Excoecaria</i>	1
		<i>Rhododendron + Cotoneaster</i>	1
		<i>Rhododendron + Salix</i>	1
		<i>Rhododendron + Sorbus</i>	1
		<i>Rosa + Caryopteris + Artemisia</i>	1
		<i>Zanthoxylum + Chrysojasminum</i>	1
		<i>Zanthoxylum + Rhamnus</i>	1
	EBS	<i>Daphne + Quercus</i>	1
		<i>Dodonaea</i>	1
		<i>Gaultheria</i>	1
		<i>Lithocarpus + Castanopsis</i>	1
		<i>Osteomeles + Fargesia</i>	1
		<i>Pistacia</i>	1
		<i>Quercus</i>	12
		<i>Rhododendron</i>	22
	BS	<i>Fargesia</i>	2
Grassland	TG	<i>Carex</i>	1
		<i>Carex + Kobresia</i>	2
		<i>Festuca</i>	1
		<i>Festuca + Carex</i>	1
		<i>Festuca + Kobresia</i>	1
		<i>Kobresia</i>	25
		<i>Kobresia + Argentina</i>	1

	<i>Kobresia + Potentilla</i>	1
	<i>Poa</i>	1
	<i>Poa + Bistorta</i>	1
RG	<i>Carex</i>	5
	<i>Carex + Kobresia</i>	2
	<i>Carex + Kobresia + Blysmus</i>	1
	<i>Carex + Potentilla</i>	1
	<i>Carex + Stipa</i>	1
	<i>Trichophorum</i>	1
FG	<i>Anaphalis</i>	1
	<i>Anaphalis + Argentina</i>	1
	<i>Androsace</i>	1
	<i>Argentina</i>	5
	<i>Artemisia</i>	1
	<i>Bistorta</i>	1
	<i>Bistorta + Trollius</i>	1
	<i>Eremogone</i>	1
	<i>Salix + Anemone</i>	1
	<i>Sibbaldia</i>	1
SSG	<i>Artemisia</i>	2

606 DNF, deciduous needleleaf forest; DENF, mixed deciduous and evergreen needleleaf forest; ENF,  
607 evergreen needleleaf forest; NBF, mixed needleleaf and broadleaf forest; DBF, deciduous broadleaf  
608 forest; EDBF, mixed evergreen and deciduous broadleaf forest; EBF, evergreen broadleaf forest; RF,  
609 rainforest; ENS, evergreen needleleaf shrubland; NBS, needleleaf and broadleaf shrubland; DBS,  
610 deciduous broadleaf shrubland; EDBS, evergreen and deciduous broadleaf shrubland; EBS,  
611 evergreen broadleaf shrubland; BS, bamboo shrubland; TG, tussock grassland; RG, rhizome  
612 grassland; FG, forb grassland; SSG, semi-shrubby grassland.

613 Forest vegetation formation group includes eight vegetation formations: deciduous  
614 needleleaf forest (DNF), mixed deciduous and evergreen needleleaf forest (DENF),  
615 evergreen needleleaf forest (ENF), mixed needleleaf and broadleaf forest (NBF),  
616 deciduous broadleaf forest (DBF), mixed evergreen and deciduous broadleaf forest  
617 (EDBF), evergreen broadleaf forest (EBF), and rainforest (RF) (Table 3S4). DNF  
618 includes only one alliance (*Larix potaninii* var. *macrocarpa*) and appears at 3,732–  
619 4,136 m in the central and northwestern HDM study region. It has  $10 \pm 2$  species per  
620 plot, community height of  $10.5 \pm 3.9$  m, coverage of  $71 \pm 13\%$ , and mean DBH of  $11.9$   
621  $\pm 5.1$  cm. DENF is also rare and was recorded from a single plot in Fugong (western  
622 border between China and Myanmar) at 3,247 m. This plot contains 4 species,  
623 community height of 15.6 m, coverage of 35%, and mean DBH of 10.1 cm. ENF is

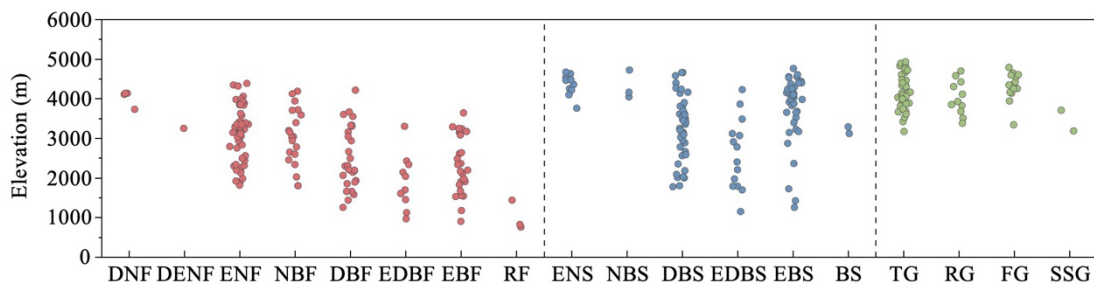
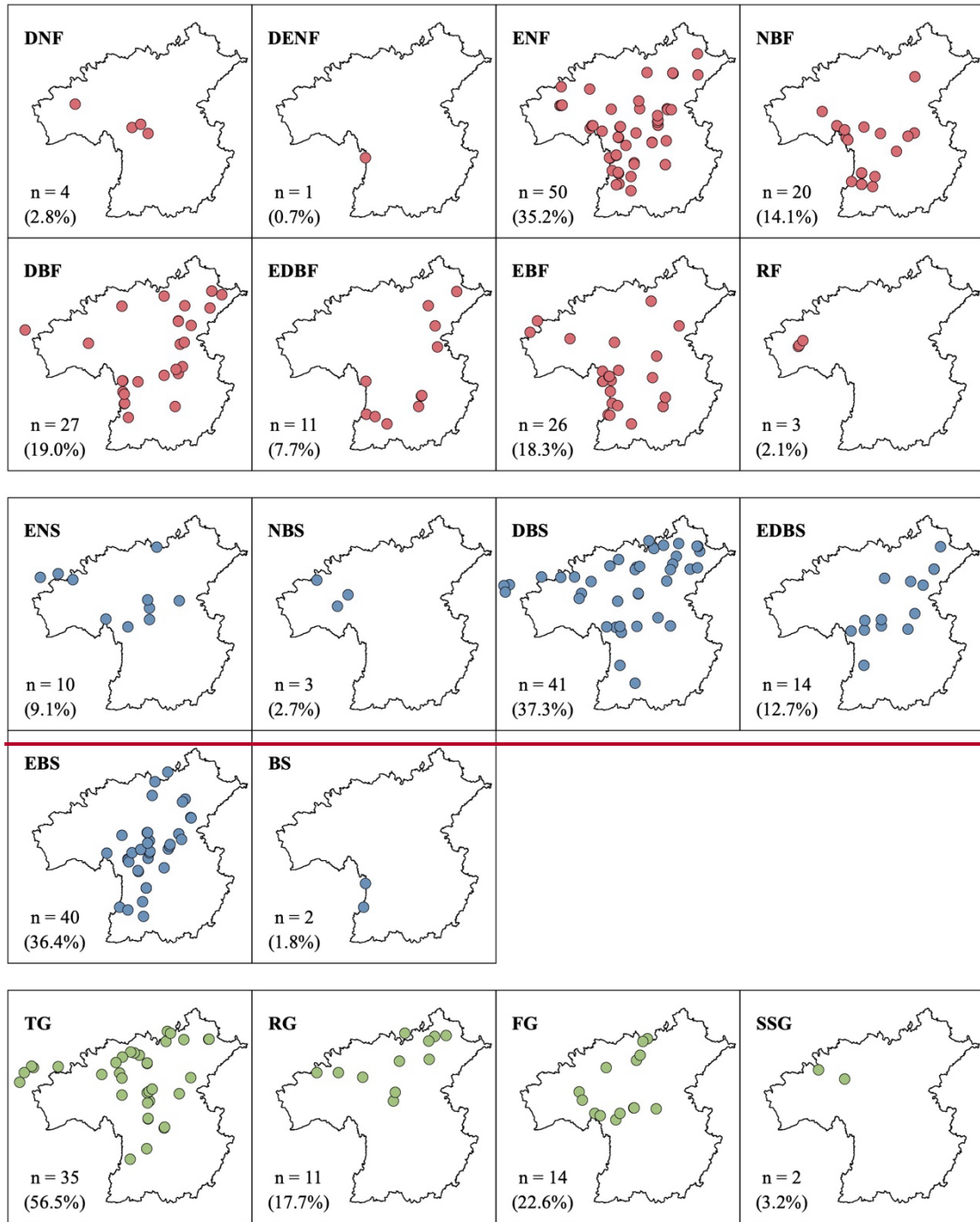
624 widespread throughout the HDM-study region at 1,809–4,377 m and is constructed by  
625 *Pinus*, *Abies*, *Picea*, *Juniperus*, and *Tsuga*. It includes 12 ± 6 species per plot,  
626 community height of 16.7 ± 7.4 m, coverage of 66 ± 14%, and mean DBH of 17.1 ±  
627 11.6 cm. NBF is concentrated in the southern HDM-study region at 1,801–4,189 m and  
628 typically combines *Pinus*, *Abies* and *Picea* with broadleaf trees such as *Quercus*, *Alnus*,  
629 and *Lithocarpus*. This formation records 14 ± 7 species per plot, community height of  
630 18.9 ± 6.4 m, coverage of 68 ± 17%, and mean DBH of 16.1 ± 7.9 cm. DBF is widely  
631 distributed at 1,256–4,217 m, excluding the northwestern HDM-study region, and is  
632 commonly constructed by *Alnus*, *Betula*, *Quercus*, and *Populus*. The corresponding  
633 plot-level values are 14 ± 7 species per plot, 13.1 ± 5.5 m in community height, 76 ±  
634 13% in coverage, and 10.2 ± 5.8 cm in mean DBH. EDBF occurs patchily from the  
635 southwestern to northeastern HDM-study region at 966–3,298 m, where evergreen  
636 components mainly *Quercus* and *Castanopsis* co-occur with deciduous broadleaf taxa  
637 such as *Alnus*. It has 15 ± 6 species per plot, community height of 14.8 ± 6.4 m, coverage  
638 of 73 ± 10%, and mean DBH of 10.7 ± 5.5 cm. EBF is widespread at low to middle  
639 elevations (906–3,636 m) in the study region and is most frequently constructed by  
640 *Quercus*. This formation surveys 12 ± 5 species per plot, 14.7 ± 8.8 m in community  
641 height, 74 ± 16% in coverage, and 15.4 ± 8.8 cm in mean DBH. RF is restricted to the  
642 lowest elevations in Medog, ~~southeastern corner of Tibet region~~ northwestern part of the  
643 study region (754–1,431m) and is characterized by tropical and subtropical trees. RF  
644 plots contain 24 ± 7 species per plot, community height of 35.3 ± 11.9 m, coverage of  
645 80 ± 10%, and mean DBH of 23.3 ± 10.9 cm (Fig. 4+10; Table 3).

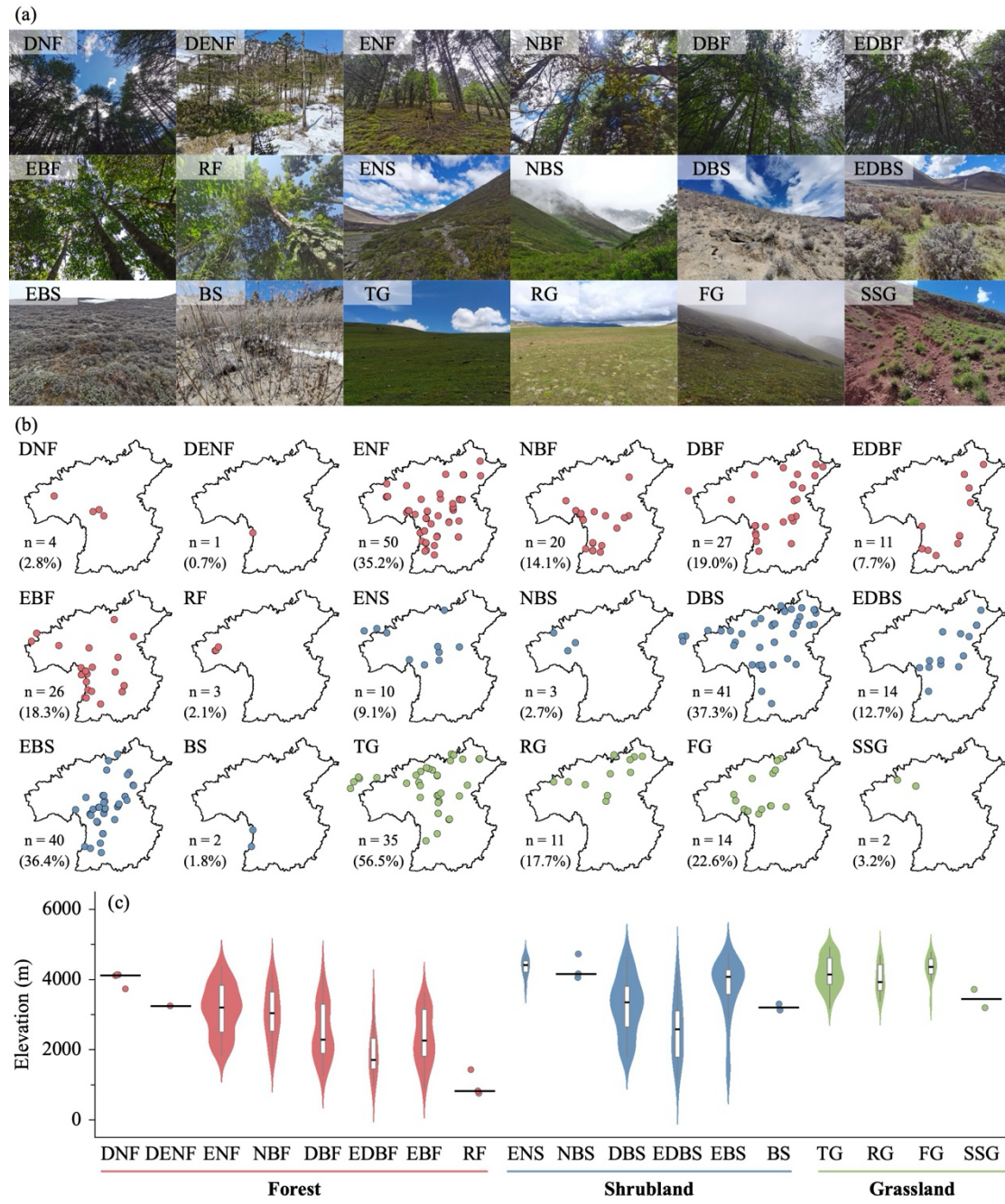
646 Shrubland vegetation formation group can be further divided into six vegetation  
647 formations: evergreen needleleaf shrubland (ENS), needleleaf and broadleaf shrubland  
648 (NBS), deciduous broadleaf shrubland (DBS), evergreen and deciduous broadleaf  
649 shrubland (EDBS), evergreen broadleaf shrubland (EBS), and bamboo shrubland (BS)  
650 (Table 3S4). ENS consists of two alliances (*Juniperus squamata* and *J. convallium*) and  
651 occurs mainly along the central and northwestern margin of the HDM-study region at  
652 3,757–4,668 m. ENS plots have 5 ± 2 species per plot, community height of 2.5 ± 2.3  
653 m, coverage of 78 ± 18%, and mean BD of 3.4 ± 1.8 cm. NBS is rare and was surveyed

654 from high-elevational area (4,044–4,720 m) in Chamdo, northwestern part of the study  
655 regioneastern Tibet, where *Juniperus* co-occurs with broadleaf shrubs including *Ribes*,  
656 *Salix*, and *Spiraea*. Its plot-level values are  $6 \pm 1$  species per plot,  $2.4 \pm 1.0$  m in  
657 community height,  $60 \pm 33\%$  in coverage, and  $2.6 \pm 1.6$  cm in mean BD. DBS is  
658 widespread across the HDM-study region at 1,772–4,662 m and is most frequently  
659 dominated by *Berberis*, *Salix*, *Rosa*, *Cotoneaster*, and *Sibiraea*. This formation includes  
660  $7 \pm 4$  species per plot, community height of  $2.7 \pm 1.7$  m, coverage of  $61 \pm 21\%$ , and  
661 mean BD of  $1.6 \pm 0.6$  cm. EDBS spans a broad elevational gradient (1,144–4,226 m)  
662 from the central to northeastern HDM-study region and features mixtures of evergreen  
663 (e.g., *Rhododendron* and *Daphne*) with deciduous components (e.g., *Rosa* and  
664 *Zanthoxylum*). EDBS plots contain  $10 \pm 6$  species per plot, community height of  $3.6 \pm$   
665  $3.1$  m, coverage of  $62 \pm 22\%$ , and mean BD of  $1.9 \pm 1.2$  cm. EBS is widely distributed  
666 from the southwestern to northeastern HDM-study region at 1,257–4,758 m and is  
667 commonly dominated by *Rhododendron* and *Quercus*. It has  $5 \pm 4$  species per plot,  
668 community height of  $2.5 \pm 2.3$  m, coverage of  $69 \pm 17\%$ , and mean BD of  $1.6 \pm 1.1$  cm.  
669 BS is uncommon in the dataset and was found in Yunnan Province at 3,120–3,290 m  
670 and includes two alliances (*Fargesia gongshanensis* and *F. melanostachys*). BS plots  
671 record  $5 \pm 4$  species per plot, community height of  $5.4 \pm 2.9$  m, coverage of  $68 \pm 11\%$ ,  
672 and mean BD of  $2.7 \pm 1.1$  cm (Fig. 4+10; Table 3).

673 Grassland vegetation formation group comprises four vegetation formations:  
674 tussock grassland (TG), rhizome grassland (RG), forb grassland (FG), and semi-shrub  
675 grassland (SSG) (Table 3S4). TG is widespread across the HDM-study region at 3,168–  
676 4,932 m and is strongly dominated by *Kobresia*, especially the widespread alpine  
677 meadow species *K. pygmaea* (24 plots). This formation has  $12 \pm 4$  species per plot,  
678 community height of  $0.061 \pm 0.033$  m, and coverage of  $81 \pm 15\%$ . RG occurs mainly  
679 in the northern HDM-study region at 3,379–4,701 m and is represented by *Carex*, with  
680 *C. enervis* frequently recorded. It contains  $14 \pm 5$  species per plot, community height of  
681  $0.108 \pm 0.102$  m, and coverage of  $79 \pm 25\%$ . FG is concentrated from the central to  
682 northern HDM-study region at 3,345–4,784 m and is characterized by forb constructed  
683 communities, with *Argentina* as a common genus. Its plot-level values are  $11 \pm 6$

684 species per plot,  $0.079 \pm 0.055$  m in community height, and  $77 \pm 16\%$  in coverage. SSG  
685 is rare and has a single alliance (*Artemisia vestita*), observed in dry-hot valleys in the  
686 northwestern HDM-study region at 3,186–3,710 m. The alliance has  $5 \pm 3$  species per  
687 plot, community height of  $0.300 \pm 0.283$  m, and coverage of  $50 \pm 28\%$  (Fig. 4+10; Table  
688 3).





690

691 **Figure 410.** Representative photographs (a), Horizontal distribution (b), and elevational  
 692 distribution (c) of vegetation formations in the HDM-Plot dataset. Red, blue, and green dots-points  
 693 represent forest, shrubland, and grassland vegetation formations-group, respectively. n denotes the  
 694 number of plots for each vegetation formation, and values in parentheses indicate the proportion of  
 695 the corresponding formation group. Violin plots with embedded boxplots are shown for vegetation  
 696 formations represented by at least five plots, whereas formations with fewer than five plots are  
 697 displayed as individual points only. Black horizontal lines reflect median elevation. DNF, deciduous  
 698 needleleaf forest; DENF, mixed deciduous and evergreen needleleaf forest; ENF, evergreen  
 699 needleleaf forest; NBF, mixed needleleaf and broadleaf forest; DBF, deciduous broadleaf forest;  
 700 EDBF, mixed evergreen and deciduous broadleaf forest; EBF, evergreen broadleaf forest; RF,  
 701 rainforest; ENS, evergreen needleleaf shrubland; NBS, needleleaf and broadleaf shrubland; DBS,

702 deciduous broadleaf shrubland; EDBS, evergreen and deciduous broadleaf shrubland; EBS,  
 703 evergreen broadleaf shrubland; BS, bamboo shrubland; TG, tussock grassland; RG, rhizome  
 704 grassland; FG, forb grassland; and SSG, semi-shrubby grassland.

705 **Table 3** Summary of community characteristics and structure in the HDM-Plot dataset

<u>Formations</u>	<u>SR</u>	<u>Community height (m)</u>	<u>Community Coverage (%)</u>	<u>DBH or BD (cm)</u>
<u>DNF</u>	<u>10 ± 2</u>	<u>10.5 ± 3.9</u>	<u>71 ± 13</u>	<u>11.9 ± 5.1</u>
<u>DENF</u>	<u>4</u>	<u>15.6</u>	<u>35</u>	<u>10.1</u>
<u>ENF</u>	<u>12 ± 6</u>	<u>16.7 ± 7.4</u>	<u>66 ± 14</u>	<u>17.1 ± 11.6</u>
<u>NBF</u>	<u>14 ± 7</u>	<u>18.9 ± 6.4</u>	<u>68 ± 17</u>	<u>16.1 ± 7.9</u>
<u>DBF</u>	<u>14 ± 7</u>	<u>13.1 ± 5.5</u>	<u>76 ± 13</u>	<u>10.2 ± 5.8</u>
<u>EDBF</u>	<u>15 ± 6</u>	<u>14.8 ± 6.4</u>	<u>73 ± 10</u>	<u>10.7 ± 5.5</u>
<u>EBF</u>	<u>12 ± 5</u>	<u>14.7 ± 8.8</u>	<u>74 ± 16</u>	<u>15.4 ± 8.8</u>
<u>RF</u>	<u>24 ± 7</u>	<u>35.3 ± 11.9</u>	<u>80 ± 10</u>	<u>23.3 ± 10.9</u>
<u>ENS</u>	<u>5 ± 2</u>	<u>2.5 ± 2.3</u>	<u>78 ± 18</u>	<u>3.4 ± 1.8</u>
<u>NBS</u>	<u>6 ± 1</u>	<u>2.4 ± 1.0</u>	<u>60 ± 33</u>	<u>2.6 ± 1.6</u>
<u>DBS</u>	<u>7 ± 4</u>	<u>2.7 ± 1.7</u>	<u>61 ± 21</u>	<u>1.6 ± 0.6</u>
<u>EDBS</u>	<u>10 ± 6</u>	<u>3.6 ± 3.1</u>	<u>62 ± 22</u>	<u>1.9 ± 1.2</u>
<u>EBS</u>	<u>5 ± 4</u>	<u>2.5 ± 2.3</u>	<u>69 ± 17</u>	<u>1.6 ± 1.1</u>
<u>BS</u>	<u>5 ± 4</u>	<u>5.4 ± 2.9</u>	<u>68 ± 11</u>	<u>2.7 ± 1.1</u>
<u>TG</u>	<u>12 ± 4</u>	<u>0.061 ± 0.033</u>	<u>81 ± 15</u>	<u>/</u>
<u>RG</u>	<u>14 ± 5</u>	<u>0.108 ± 0.102</u>	<u>79 ± 25</u>	<u>/</u>
<u>FG</u>	<u>11 ± 6</u>	<u>0.079 ± 0.055</u>	<u>77 ± 16</u>	<u>/</u>
<u>SSG</u>	<u>5 ± 3</u>	<u>0.300 ± 0.283</u>	<u>50 ± 28</u>	<u>/</u>

706 Values are summarized at the plot level within each vegetation formation and are shown as mean ±  
 707 SD. SR denotes species richness per plot. DBH or BD represents the mean diameter at breast height  
 708 or basal diameter of woody species within each plot.

## 709 **5 Data availability**

710 The HDM-Plot dataset includes two components: a plot dataset and a habitat photo  
 711 dataset. The plot dataset is provided as a Microsoft Excel format containing six sheets:  
 712 1) summary (Table 4); 2) basic plot information; 3) raw plot survey data; 4) species list;

713 5) species important values; and 6) vegetation classification. The habitat photo dataset  
 714 is organized by survey period (i.e., 202203, 202205, 2023, and 2024). Photo files are  
 715 provided in JPG format, named by plot ID, and correspond to the plots in the dataset.  
 716 The dataset is publicly available through the National Tibetan Plateau / Third Pole  
 717 Environment Data Center (Jin et al., 2026; <https://doi.org/10.11888/Terre.tpdc.303394>).

718 **Table 4** Summary information of the HDM-Plot dataset.

Heading	Description	Type
Plot No	Plot number based on survey time	Code
Province	Administrative province of the plot location	Character
Longitude (°E)	Longitude in decimal degrees by GPS	Numeric
Latitude (°N)	Latitude in decimal degrees by GPS	Numeric
Elevation (m)	Elevation in decimal degrees by GPS	Integer
Disturbance intensity	Degree of disturbance recorded in the survey	Character
Plot size (m × m)	Plot size = plot length × plot width	Character
Community height (m)	Maximum <del>plant</del> -height <u>of the dominant vegetation layer in within the a</u> plot	Numeric
Community coverage (%)	Total vegetation coverage of the plot	Integer
Species richness	Number of species recorded in the plot	Integer
Latin name	Scientific name of the species (Flora of China, FOC)	Character
Growth form	Tree, shrub, climber, semi-shrub, and herb	Character
Phenological period	Phenological stage during survey (e.g., leaf period)	Character
Number of plants (clusters)	Number of individuals or clumps recorded	Integer
Height (m)	Leaf-layer height (herb) / canopy height (woody)	Numeric
FBH (cm)	Reproductive branch height (herb)	Numeric
BD (cm)	Base diameter	Numeric
DBH (cm)	Diameter at breast height	Numeric
Crown a (m)	Maximum crown width (woody)	Numeric
Crown b (m)	Crown width perpendicular to maximum axis (woody)	Numeric
Coverage (%)	Specific species coverage (herb)	Numeric

Plant status	Vitality status of the individual (e.g., dead wood)	Character
Chinese name	Chinese name of the species (FOC)	Character
Genus	Genus of the species (FOC)	Character
Family	Family of the species (FOC)	Character
Leaf phenology	Deciduous vs. Evergreen	Character
Leaf type	Broadleaf vs. needleleaf	Character
Life span	Annual, biennial, and perennial	Character
No. of plots observed	Number of plots in which the species was recorded	Integer
Layer	Vegetation layer (e.g., tree layer)	Character
IV (%)	Importance value of the species within the plot	Numeric
Vegetation formation group	Supplementary upper-level unit (e.g., forest)	Character
Vegetation formation	Upper-level unit (e.g., evergreen needleleaf forest)	Character
Alliance group	Supplementary middle-level unit (e.g., <i>Abie</i> forest)	Character
Alliance	Middle-level unit (e.g., <i>A. georgei</i> forest)	Character
Association group	Supplementary lower-level unit (e.g., <i>A. georgei</i> - shrub forest)	Character
Association	Lower-level unit ( <i>A. georgei</i> - <i>Rubus amabilis</i> forest)	Character

## 719 6 Summary

720 The HDM-Plot dataset was compiled from four extensive fieldworks conducted  
721 by our research group between 2022 and 2024. It provides detailed raw records from  
722 314 vegetation plots spanning major vegetation types in the HDM and adjacent regions,  
723 from low-elevational dry-hot valleys to subalpine and alpine areas. The dataset offers a  
724 robust, standardized data for studies of vegetation ecology, conservation planning, and  
725 ecological restoration in this biodiversity hotspot, and provides an important regional  
726 complement to global vegetation plot compilations such as the sPlot (Sabatini et al.,  
727 2021), which rarely include the vegetation plots from southwestern China and the  
728 Tibetan Plateau. The localized vegetation plot dataset can be integrated into existing  
729 global plot database of sPlot, and further contributes to large-scale synthesis.

730 Several limitations remain due to the challenging field conditions and constraints  
731 in manpower and resources. First, although the surveyed plots cover broad vegetation  
732 types, climatic space, and elevational gradients (Fig. 2), the study region, especially the  
733 HDM ~~have~~-has extremely complex topography and highly heterogeneous vegetation,  
734 and steep terrain often prevented the establishment of fully standardized plots. As a  
735 result, plot size could not always be kept uniform, and plot distribution may be uneven  
736 in some areas, which can affect representativeness and comparability. Second, given  
737 the high diversity and strong spatial turnover of species composition, individual plots  
738 may not fully capture the regional variability, potentially producing sampling bias.  
739 Third, some plot attributes, such as plant height, crown width, and coverage, were  
740 visually estimated in the field and may therefore be subject to observer uncertainty.  
741 Nevertheless, these limitations should be viewed in the context of field-based  
742 vegetation surveys in a topographically complex and highly heterogeneous mountain  
743 region. assembling Assembling a large, structurally detailed plot dataset under harsh  
744 field conditions represents a vital contribution. More importantly, we believe that the  
745 dataset remains a valuable community resource for large-scale mountain vegetation  
746 studies, as it provides standardized and openly accessible plot-level records from highly  
747 heterogeneous and relatively underrepresented mountain region. ,and wWe expect the  
748 HDM-Plot dataset to provide a valuable reference for ongoing and future efforts of  
749 vegetation reassessment and ecological research across the region. \_

750 Compared with our previously published dataset on the Tibetan Plateau (Jin et al.,  
751 2022), the HDM-Plot dataset fills a key geographic gap on the southeastern Plateau and  
752 demonstrates enhanced representativeness about plot distribution, species richness, and  
753 vegetation types. Plots are not restricted to areas along major roads, but also extend into  
754 accessible valleys and pathways. This is the first comprehensive vegetation plot dataset  
755 for the HDM and adjacent regions to our knowledge with broad spatial coverage and  
756 representation of diverse vegetation types. In addition to raw species composition  
757 records, the dataset provides standardized geographic coordinates, species list, and  
758 hierarchical vegetation classifications.

759 The vegetation classification in the HDM-Plot dataset follows the revised

760 vegetation classification system of China (Guo et al., 2020), emphasizing field-based  
761 community physiognomy, vertical structure, constructive species, and species  
762 importance values. This approach provides a field-based and nationally consistent  
763 framework for vegetation classification and future comparison with the *Vegegraphy of*  
764 *China*. During vegetation classification, we observed shrubland communities in which  
765 co-constructive species differ in leaf type and phenology, analogous to mixed forests.  
766 For example, shrublands jointly dominated by *Juniperus* and *Rhododendron* combine  
767 needleleaf and broadleaf components and may include evergreen and deciduous  
768 elements. Accordingly, we introduced two shrubland vegetation formations within the  
769 Guo et al. (2020) scheme: (a) needleleaf and broadleaf shrubland, and (b) evergreen and  
770 deciduous broadleaf shrubland. Similarly, in grasslands, co-constructive species often  
771 belong to different functional groups (e.g., tussock, rhizome, and forb), which are not  
772 always clearly separated in the current classification framework. We therefore retained  
773 multiple co-constructive species in alliance naming, while identifying the vegetation  
774 formation according to the life form of the species with the highest IV. For example,  
775 *Kobresia pygmaea* + *Potentilla saundersiana* grassland alliance was classified as a  
776 tussock grassland vegetation formation.

777 As a complementary assessment, we further numerically classified vegetation  
778 from the HDM-Plot dataset based on species composition using TWINSpan (Fig. S3).  
779 The first division broadly separated alpine grassland plots from non-alpine grassland  
780 plots, consistent with the major physiognomic contrast in the dataset. However, finer  
781 divisions did not always correspond to the field-based vegetation formations, probably  
782 reflecting local species turnover, rare taxa, and uneven sampling among vegetation  
783 types. Therefore, quantitative classification provides a useful complementary  
784 perspective, but the field-based classification following Guo et al. (2020) remains the  
785 primary framework for this data paper. These plot-based findings and standardized data  
786 provide support for the ongoing revision of China's vegetation classification system  
787 (Guo et al., 2020) and for the update of *Vegegraphy of China* (Fang et al., 2020). The  
788 ecological environment of southwestern China is highly fragile and increasingly  
789 exposed to human pressures, with limited capacity for natural recovery. Updated and

790 standardized baseline data is therefore essential for guiding conservation, ecological  
791 planning, and restoration strategies, and for supporting biodiversity assessments and  
792 ecosystem management in this global hotspot under ongoing and future climate change.  
793 More broadly, the HDM-Plot dataset can also contribute to global vegetation ecology  
794 by improving the representation of Asian mountain ecosystems in plot-based research.  
795 Vegetation plots from southwestern China and the southeastern Tibetan Plateau remain  
796 relatively rare in global compilations, despite the high biodiversity and strong  
797 environmental heterogeneity of this region. By providing standardized field-based  
798 records from this underrepresented mountain system, the dataset can support cross-  
799 regional comparisons and large-scale syntheses of vegetation classification,  
800 biodiversity patterns, community structure, and ecosystem responses to environmental  
801 change.

802 **Author contributions.** JN conceived the study. JN and XM led the field works. YJ, LY,  
803 CY, XH, HX, YH, KW, and SS participated in vegetation survey. SS processed the  
804 climate maps. YJ and LY processed the dataset, performed the analyses and wrote the  
805 first draft. JN, XM and YJ improved the manuscript. All the authors approved the final  
806 version of the submitted manuscript.

807 **Competing interests.** The (co-) authors declare that they have no conflict of interest.

808 **Disclaimer.** Publisher's note: Copernicus Publications remains neutral with regard to  
809 jurisdictional claims in published maps and institutional affiliations.

810 **Acknowledgements.** The authors sincerely thank Qiuting Chen, Tingting Chen,  
811 Zhichao Chen, Tao Fang, Chuting Hu, Saijing Liu, Xiaoling Lu, Chenling Wang,  
812 Haoyan Wang, Jie Xia, Yang Yang, Pingqian Ye, Bohan Zheng, Yawen Zheng, and Yan  
813 Zhou from Zhejiang Normal University for their help in the field survey, Dashan He  
814 from Sichuan University for helping with specimen identification, and Ke Guo from  
815 Institute of Botany, the Chinese Academy of Sciences for providing assistance in  
816 vegetation classification.

817 **Financial support.** This work was supported by the Second Tibetan Plateau Scientific  
818 Expedition and Research Program (grant no. 2019QZKK0402).

819 **References**

- 820 Chi, X. F., Zhang, F. Q., Gao, Q. B., Xing, R., and Chen, S. L.: Genetic structure and eco-  
821 geographical differentiation of *Lancea tibetica* in the Qinghai-Tibetan Plateau, *Genes*, 10, 97,  
822 <https://doi.org/10.3390/genes10020097>, 2019.
- 823 Ding, W. N., Ree, R. H., Spicer, R. A., and Xing, Y. W.: Ancient orogenic and monsoon-driven  
824 assembly of the world's richest temperate alpine flora, *Science*, 369, 578–581,  
825 <https://doi.org/10.1126/science.abb4484>, 2020.
- 826 Editorial Committee of the Flora of China: *Reipublicae Popularis Sinicae*, 80 volumes, Science  
827 Press, Beijing, 1959–2004.
- 828 Editorial Committee of Vegetation of China: *Vegetation of China*, Science Press, Beijing, 1980.
- 829 Editorial Committee of Vegetation Map of China, Chinese Academy of Sciences: *Vegetation of*  
830 *China and Its Geographical Pattern – Illustration of the Vegetation Map of the People's*  
831 *Republic of China (1:1,000,000)*, Geology Press, Beijing, 2007a.
- 832 Editorial Committee of Vegetation Map of China, Chinese Academy of Sciences: *Vegetation Map*  
833 *of the People's Republic of China (1:1,000,000)*, Geology Press, Beijing, 2007b.
- 834 Fang, J. Y., Wang, X. P., Shen, Z. H., Tang, Z. Y., He, J. S., Yu, D., Jiang, Y., Wang, Z. H., Zheng,  
835 C. Y., Zhu, J. L., and Guo, Z. D.: Methods and protocols for plant community inventory, *Biodiv.*  
836 *Sci.*, 17, 533–548, <https://doi.org/10.3724/SP.J.1003.2009.09253>, 2009.
- 837 Fang, J. Y., Guo, K., Wang, G. H., Tang, Z. Y., Xie, Z. Q., Shen, Z. H., Wang, R. Q., Qiang, S., Liang,  
838 C. Z., Da, L. J., and Yu, D.: Vegetation classification system and classification of vegetation  
839 types used for the compilation of vegetation of China, *Chin. J. Plant Ecol.*, 44, 96–110, 2020.
- 840 Farr, T. G., Rosen, P. A., Caro, E., Crippen, R., Duren, R., Hensley, S., Kobrick, M., Paller, M.,  
841 Rodriguez, E., Roth, L., Seal, D., Shaffer, S., Shimada, J., Umland, J., Werner, M., Oskin, M.,  
842 Burbank, D., and Alsdorf, D.: The Shuttle Radar Topography Mission, *Rev. Geophys.*, 45:  
843 RG2004, <https://doi.org/10.1029/2005RG000183>, 2007.
- 844 Gao, B. C., Fang, W. P., Kong, X. X., Xu, J. M., Guan, Z. T., Yang, J. L., Xiong, J. H., Yi, T. P., Wu,  
845 Y. T., Tan, and Z. M.: *Flora of Sichuan*, Sichuan People's Publishing House, Chengdu, 1981.
- 846 Guo, K., Fang, J. Y., Wang, G. H., Tang, Z. Y., Xie, Z. Q., Shen, Z. H., Wang, R. Q., Qiang, S., Liang,  
847 C. Z., Da, L. J., and Yu, D.: A revised scheme of vegetation classification system of China,

848 Chin. J. Plant Ecol., 44, 111–127, <https://doi.org/10.17521/cjpe.2019.0271>, 2020.

849 He, Y. L., Xiong, Q. L., Yu, L., Yan, W. B., and Qu, X. X.: Impact of climate change on potential  
850 distribution patterns of alpine vegetation in the Hengduan Mountains region, China, Mt. Res.  
851 Dev., 40, R48–R54, <https://doi.org/10.1659/MRD-JOURNAL-D-20-00010.1>, 2020.

852 [Hu, X. F., Shi, S. L., Zhou, B. R., and Ni, J.: A 1 km monthly dataset of historical and future climate](#)  
853 [changes over China. Sci. Data, 12, 436, https://doi.org/10.1038/s41597-025-04761-y, 2025.](#)

854 iFlora Initiative of Kunming Institute of Botany, Chinese Academy of Sciences: A Dictionary of the  
855 Families and Genera of Chinese Vascular Plants, Science Press, Beijing, 2018.

856 Integrated Scientific Expedition to Qinghai-Tibet Plateau, Chinese Academy of Sciences: Flora  
857 Xizangica, 5 volumes, Science Press, Beijing, 1983–1987.

858 Integrated Scientific Expedition to Qinghai-Tibet Plateau, Chinese Academy of Sciences: Physical  
859 Geography of Hengduan Mountains, Science Press, Beijing, 1997.

860 Jin, Y. L., Wang, H. Y., Wei, L. F., Hou, Y., Hu, J., Wu, K., Xia, H. J., Xia, J., Zhou, B. R., Li, K.,  
861 and Ni, J.: A plot-based dataset of plant community on the Qingzang Plateau, Chin. J. Plant  
862 Ecol., 46, 846–854, <https://doi.org/10.17521/cjpe.2022.0174>, 2022.

863 Jin, Y. L., Yang, L. Y. Y., Hu, X. F., Yang, C., Xia, H. J., Hou, Y., Wu, K., Mao, X. X., Ni, J.: A plot-  
864 based plant community dataset in the Hengduan Mountains (2022-2024), National Tibetan  
865 Plateau / Third Pole Environment Data Center, <https://doi.org/10.11888/Terre.tpdc.303394>,  
866 2026.

867 Jin, Z. Z.: The Features of Floras in the Dry-hot and Dry-warm Valleys in Yunnan and Sichuan  
868 Provinces, Yunnan Science and Technology Press, Kunming, 2002.

869 Jin, Z. Z., and Ou, X. K.: Yuanjiang, Nujiang, Jinshajiang, Lancangjiang Vegetation of Dry Valley,  
870 Yunnan University Press & Yunnan Science and Technology Press, Kunming, 2000.

871 Kunming Institute of Botany, Chinese Academy of Sciences: Flora of Yunnan, 21 volumes, Science  
872 Press, Beijing, 1977–2006.

873 Li, D. J.: The primary characteristics of flora in the Hengduan Mountainous regions, Mt. Res., 6,  
874 147–152, <https://doi.org/10.16089/j.cnki.1008-2786.1988.03.003>, 1988.

875 Li, X. W.: Floristic statistics and analyses of seed plants from China, Acta Bot. Yunnan., 18, 363–  
876 384, 1996.

877 Liang, Q. L., Xu, X. T., Mao, K. S., Wang, M. C., Wang, K., Xi, Z. X., and Liu, J. Q.: Shifts in plant

878 distributions in response to climate warming in a biodiversity hotspot, the Hengduan  
879 Mountains, *J. Biogeogr.*, 45, 1334–1344, <https://doi.org/10.1111/jbi.13229>, 2018.

880 Liu, Y., Li, P., Xu, Y., Shi, S. L., Ying, L. X., Zhang, W. J., Peng, P. H., and Shen, Z. H.: Quantitative  
881 classification and ordination for plant communities in dry valleys of Southwest China, *Biodiv.*  
882 *Sci.*, 24, 378–388, <https://doi.org/10.17520/biods.2015241>, 2016a.

883 Liu, Y., Zhu, X. X., Shen, Z. H., and Sun, H.: Flora compositions and spatial differentiations of  
884 vegetation in dry valleys of Southwest China, *Biodiv. Sci.*, 24, 367–377,  
885 <https://doi.org/10.17520/biods.2015240>, 2016b.

886 Myers, N., Mittermeier, R. A., Mittermeier, C. G., da Fonseca, G. A. B., and Kent, J.: Biodiversity  
887 hotspots for conservation priorities, *Nature*, 403, 853–858, <https://doi.org/10.1038/35002501>,  
888 2000.

889 Nan, X., Li, A. N., and Deng, W.: Data set of “Digital Mountain Map of China” (2015), National  
890 Tibetan Plateau / Third Pole Environment Data Center,  
891 <https://doi.org/10.11888/Terre.tpdc.272523>, 2022.

892 Piao, S. L., Zhang, X. Z., Wang, T., Liang, E. Y., Wang, S. P., Zhu, J. T., and Niu, B.: Responses and  
893 feedback of the Tibetan Plateau’s alpine ecosystem to climate change, *Chin. Sci. Bull.*, 64,  
894 2842–2855, <https://doi.org/10.1360/TB-2019-0074>, 2019.

895 Sabatini, F. M., Lenoir, J., Hattab, T., Arnst, E. A., Chytrý, M., Dengler, J., De Ruffray, P., Hennekens,  
896 S. M., Jandt, U., Jansen, F., Jiménez-Alfaro, B., Kattge, J., Levesley, A., Pillar, V. D., Purschke,  
897 O., Sandel, B., Sultana, F., Aavik, T., Ačić, S., Acosta, A. T. R., Agrillo, E., Alvarez, M.,  
898 Apostolova, I., Arfin Khan, M. A. S., Arroyo, L., Attorre, F., Aubin, I., Banerjee, A., Bauters,  
899 M., Bergeron, Y., Bergmeier, E., Biurrun, I., Bjorkman, A. D., Bonari, G., Bondareva, V.,  
900 Brunet, J., Čarni, A., Casella, L., Cayuela, L., Černý, T., Chepinoga, V., Csiky, J., Čušterevska,  
901 R., De Bie, E., de Gasper, A. L., De Sanctis, M., Dimopoulos, P., Dolezal, J., Dziuba, T., El-  
902 Sheikh, M. A. E.-R. M., Enquist, B., Ewald, J., Fazayeli, F., Field, R., Finckh, M., Gachet, S.,  
903 Galán-de-Mera, A., Garbolino, E., Gholizadeh, H., Giorgis, M., Golub, V., Alsos, I. G., Grytnes,  
904 J.-A., Guerin, G. R., Gutiérrez, A. G., Haider, S., Hatim, M. Z., Hérault, B., Hinojos Mendoza,  
905 G., Hölzel, N., Homeier, J., Hubau, W., Indreica, A., Janssen, J. A. M., Jedrzejek, B., Jentsch,  
906 A., Jürgens, N., Kaçki, Z., Kapfer, J., Karger, D. N., Kavgacı, A., Kearsley, E., Kessler, M.,  
907 Khanina, L., Killeen, T., Korolyuk, A., Kreft, H., Köhl, H. S., Kuzemko, A., Landucci, F.,

908 Lengyel, A., Lens, F., Lingner, D. V., Liu, H., Lysenko, T., Mahecha, M. D., Marcenò, C.,  
 909 Martynenko, V., Moeslund, J. E., Monteagudo Mendoza, A., Mucina, L., Müller, J. V.,  
 910 Munzinger, J., Naqinezhad, A., Noroozi, J., Nowak, A., Onyshchenko, V., Overbeck, G. E.,  
 911 Pärtel, M., Pauchard, A., Peet, R. K., Peñuelas, J., Pérez-Haase, A., Peterka, T., Petřík, P., Peyre,  
 912 G., Phillips, O. L., Prokhorov, V., Rašomavičius, V., Revermann, R., Rivas-Torres, G., Rodwell,  
 913 J. S., Ruprecht, E., Rūsiņa, S., Samimi, C., Schmidt, M., Schrodte, F., Shan, H., Shirokikh, P.,  
 914 Šibík, J., Šilc, U., Sklenář, P., Škvorc, Ž., Sparrow, B., Sperandii, M. G., Stančić, Z., Svenning,  
 915 J.-C., Tang, Z., Tang, C. Q., Tsiripidis, I., Vanselow, K. A., Vásquez Martínez, R., Vassilev, K.,  
 916 Vélez-Martín, E., Venanzoni, R., Vibrans, A. C., Violle, C., Virtanen, R., von Wehrden, H.,  
 917 Wagner, V., Walker, D. A., Waller, D. M., Wang, H.-F., Wesche, K., Whitfeld, T. J. S., Willner,  
 918 W., Wisser, S. K., Wohlgemuth, T., Yamalov, S., Zobel, M., and Bruelheide, H.: sPlotOpen – An  
 919 environmentally balanced, open-access, global dataset of vegetation plots, *Glob. Ecol.*  
 920 *Biogeogr.*, 30, 1740–1764, <https://doi.org/10.1111/geb.13346>, 2021.

921 Shen, Z. H., Liu, Z. L., and Wu, J.: Altitudinal pattern of flora on the eastern slope of Mt. Gongga,  
 922 *Biodiv. Sci.*, 12, 89–98, <https://doi.org/10.17520/biods.2004011>, 2004.

923 Sherman, R., Mullen, R., Li, H. M., Fang, Z. D., and Wang, Y.: Spatial patterns of plant diversity  
 924 and communities in alpine ecosystems of the Hengduan Mountains, northwest Yunnan, China,  
 925 *J. Plant Ecol.*, 1, 117–136, <https://doi.org/10.1093/jpe/rtn012>, 2008.

926 Sloan, S., Jenkins, C. N., Joppa, L. N., Gaveau, D. L. A., and Laurance, W. F.: Remaining natural  
 927 vegetation in the global biodiversity hotspots, *Biol. Conserv.*, 177, 12–24,  
 928 <https://doi.org/10.1016/j.biocon.2014.05.027>, 2014.

929 Sun, H., Zhang, J. W., Deng, T., and Boufford, D. E.: Origins and evolution of plant diversity in the  
 930 Hengduan Mountains, *Plant Divers.*, 39, 161–166, <https://doi.org/10.1016/j.pld.2017.09.004>,  
 931 2017.

932 Wang, G. H., Fang, J. Y., Guo, K., Xie, Z. Q., Tang, Z. Y., Shen, Z. H., Wang, R. Q., Wang, X. P.,  
 933 Wang, D. L., Qiang, S., Yu, D., Peng, S. L., Da, L. J., Liu, Q., and Liang, C. Z.: Contents and  
 934 protocols for the classification and description of vegetation formations, alliances and  
 935 associations of vegetation of China, *Chin. J. Plant Ecol.*, 44, 128–178,  
 936 <https://doi.org/10.17521/cjpe.2019.0272>, 2020.

937 Wu, S. H., Pan, T., Cao, J., He, D. M., and Xiao, Z. N.: Barrier-corridor effect of longitudinal range-

938 gorge terrain on monsoons in Southwest China, *Geogr. Res.*, 31, 1–13,  
939 <https://doi.org/10.11821/yj2012010001>, 2012.

940 Wu, Z. Y.: The areal-types of Chinese genera of seed plants. *Acta Bot. Yunnan.*, Suppl. IV, 1–139,  
941 1991.

942 Wu, Z. Y., Zhou, Z. K., Li, D. Z., Peng, H., and Sun, H.: The areal-types of the world families of  
943 seed plants, *Acta Bot. Yunnan.*, 25, 245–257, 2003.

944 Xing, Y. W., and Ree, R. H.: Uplift-driven diversification in the Hengduan Mountains, a temperate  
945 biodiversity hotspot, *P. Natl. Acad. Sci. USA*, 114, E3444–E3451,  
946 <https://doi.org/10.1073/pnas.1616063114>, 2017.

947 Xu, B., Li, Z. M., and Sun, H.: Plant diversity and floristic characters of the alpine subnival belt  
948 flora in the Hengduan Mountains, SW China, *J. Syst. Evol.*, 52, 271–279,  
949 <https://doi.org/10.1111/jse.12037>, 2014.

950 Xu, C. D., Feng, J. M., Wang, X. P., and Yang, X.: Vertical distribution patterns of plant species  
951 diversity in northern Mt. Gaoligong, Yunnan Province, *Chin. J. Ecol.*, 27, 323–330, 2008.

952 Yang, J. D., Zhang, Z. M., Shen, Z. H., Ou, X. K., Geng, Y. P., and Yang, M. Y.: Review of research  
953 on the vegetation and environment of dry-hot valleys in Yunnan, *Biodiv. Sci.*, 24, 462–474,  
954 <https://doi.org/10.17520/biods.2015251>, 2016.

955 Yang, Q. Y. and Zheng, D.: An outline of physico-geographic regionalization of the Hengduan  
956 Mountains region, *Mt. Res.*, 7, 56–64, <https://doi.org/10.16089/j.cnki.1008-2786.1989.01.010>,  
957 1989.

958 Yang, Y., Han, J., Liu, Y., Zhong-Yong, C. R., Shi, S. L., Si-Na, C. L., Xu, Y., Ying, L. X., Zhang,  
959 W. J., and Shen, Z. H.: A comparison of the altitudinal patterns in plant species diversity within  
960 the dry valleys of the Three Parallel Rivers region, northwestern Yunnan, *Biodiv. Sci.*, 24, 440–  
961 452, <https://doi.org/10.17520/biods.2015361>, 2016.

962 Yao, Y. H., Zhang, B. P., Han, F., and Pang, Y.: Diversity and geographical pattern of altitudinal belts  
963 in the Hengduan Mountains in China, *J. Mt. Sci.*, 7, 123–132, <https://doi.org/10.1007/s11629-010-1011-9>, 2010.

964

965 Yin, L., Dai, E. F., Zheng, D., Wang, Y. H., Ma, L., and Tong, M.: What drives the vegetation  
966 dynamics in the Hengduan Mountain region, southwest China: climate change or human  
967 activity?, *Ecol. Indic.*, 112, 106013, <https://doi.org/10.1016/j.ecolind.2019.106013>, 2020.

968 Yu, H. B., Miao, S. Y., Xie, G. W., Guo, X. Y., Chen, Z., and Favre, A.: Contrasting floristic diversity  
969 of the Hengduan Mountains, the Himalayas and the Qinghai-Tibet Plateau sensu stricto in  
970 China, *Front. Ecol. Evol.*, 8, 136, <https://doi.org/10.3389/fevo.2020.00136>, 2020.

971 Yu, Y. D., Liu, L. H., and Zhang, J. H.: Vegetation regionalization of the Hengduan Mountains region,  
972 *Mt. Res.*, 7, 47–55, <https://doi.org/10.16089/j.cnki.1008-2786.1989.01.009>, 1989.

973 Zhang, H. N., Zou, W., Chen, Z., He, L. J., Peng, X. F., Wang, G. Y., Peng, P. H., Li, J. J., and Shi,  
974 S. L.: Distribution pattern of plant communities and its relationship with environmental factors  
975 in eastern Xizang, China, *Chin. J. Appl. Environ. Biol.*, 29, 1289–1297,  
976 <https://doi.org/10.19675/j.cnki.1006-687x.2022.10037>, 2023.

977 Zhang, R. Z., Zheng, D., Yang, Q. Y., and Liu, Y. H.: *Physical Geography of Hengduan Mountains*,  
978 Science Press, Beijing, 1997.

979 Zhang, S.R.: *Carex*. In: Hong, D.Y., Sun, H., Watson, M., Wen, J., Zhang, X.C. (eds), *Flora of Pan-*  
980 *Himalaya*, Vol. 12, Science Press, Beijing, 2020.

981 Zhang, X. Q., Xu, X. M., Li, X., Cui, P., and Zheng, D.: A new scheme of climate-vegetation  
982 regionalization in the Hengduan Mountains region, *Sci. China Earth Sci.*, 67, 751–768,  
983 <https://doi.org/10.1007/s11430-023-1231-0>, 2024.

984 Zhang, X. Z., Yang, Y. P., Piao, S. L., Bao, W. K., Wang, S. P., Wang, G. X., Sun, H., Luo, T. X.,  
985 Zhang, Y. J., Shi, P. L., Liang, E. Y., Shen, M. G., Wang, J. S., Gao, Q. Z., Zhang, Y. L., and  
986 Ouyang, H.: Ecological change on the Tibetan Plateau, *Chin. Sci. Bull.*, 60, 3048–3056,  
987 <https://doi.org/10.1360/N972014-01339>, 2015.

988 Zheng, D.: A comparative study on physico-geographic conditions between the Himalayas and  
989 Hengduan Mountainous regions, *Mt. Res.*, 6, 137–144, 1988.

990 Zheng, D. and Yang, Q. Y.: Some problems on physicogeographic regionalization of the Hengduan  
991 Mountains region, *Mt. Res.*, 5, 7–13, 1987.